AIMS Mathematics

https://www.aimspress.com/journal/Math

AIMS Mathematics, 11(6): 19286–19320.
DOI: 10.3934/math.2026784
Received: 08 May 2026
Revised: 19 June 2026
Accepted: 22 June 2026
Published: 30 June 2026

Research article

Stability and impact of time-delay analysis of the disability labor model

Phachara Chanosot[1], Suttida Wongkaew[1], Tawatchai Petaratip[2] and Piyapong Niamsup[1,*]

[1] Department of Mathematics, Faculty of Science, Chiang Mai University, Chiang Mai 50200, Thailand

[2] Department of Mathematics, Faculty of Science, Maejo University, Chiang Mai, 50290, Thailand

* **Correspondence:** Email: piyapong.n@cmu.ac.th.

Abstract: In this work, a Thai disability labor employment model was developed using a nonlinear delay-differential equation, with the delay term capturing policy implementation lags arising from administrative processes. In addition, we established theoretical results that guarantee the existence of equilibria and characterized the effect of implementation delays on long-term market stability. In particular, the global asymptotic stability under sufficient conditions was proved using a Lyapunov approach. To evaluate parameter influence, a normalized sensitivity analysis was conducted to identify the most significant factors for unemployment dynamics. Finally, numerical results were demonstrated in two stages. First, the numerical experiments were performed to validate the theoretical stability results. Second, the model parameters were estimated using historical Thai data for 2022–2025. To improve the model's consistency with observed data, the vacancy dynamics were refined by introducing additional variables. The proposed model provides a quantitative tool for analyzing policy delays and designing effective intervention strategies in the disability labor market.

Keywords: unemployment dynamics; delay-differential equations; global stability; sensitivity analysis; disability labor market
Mathematics Subject Classification: 34K20, 93D05

1. Introduction

Unemployment remains a critical macroeconomic challenge that significantly impacts social well-being and inclusive economic growth. Designing effective policy interventions requires a deep understanding of the complex temporal dynamics governing labor markets. Unlike classical models that assume instantaneous adjustments, real-world labor systems, particularly the disability labor market in Thailand, exhibit substantial delays due to administrative procedures and training requirements. To address this, the present study employs a system of nonlinear delay-differential equations (DDEs) to explicitly incorporate implementation lags (τ) and evaluate the long-term impact of policy interventions. A wide range of mathematical frameworks has been developed to analyze unemployment dynamics. Early studies primarily focused on qualitative stability analysis of socio-economic interactions [1–3]. More recent research has shifted toward delay-differential equation (DDE) models, which provide a more realistic representation of policy implementation lags and labor market adjustments [4–6]. In parallel, sensitivity analysis has been increasingly used to identify key drivers of system behavior [7, 8], while optimal control approaches have been proposed to design cost-effective intervention strategies [9–11].

Collectively, these developments highlight the importance of integrating stability analysis, delay effects, and parameter sensitivity within a unified modeling framework. Foundational work by Misra and Singh [5, 12] introduced time delays in vacancy creation to account for financial constraints and delayed policy responses. This framework was extended by Harding and Neamtu [13], who incorporated migration effects and distributed delays to capture labor mobility and gradual policy impacts. However, many subsequent studies, including optimal control formulations [10], continue to assume instantaneous policy effects ($\tau = 0$), thereby overlooking the critical role of implementation delays in shaping system stability. This gap motivates the need for a more realistic delay-based analysis of labor market dynamics. Recent contributions have further enriched unemployment modeling by incorporating sector-specific mechanisms and policy structures. For example, Petaratip and Niamsup [6] modeled delayed vacancy creation based on lagged government data, while Singh et al. [8] identified industrialization as a stabilizing factor. Somma et al. [11] emphasized vocational education as a key control variable, and Misra et al. [7] highlighted the buffering role of the informal sector. These studies reflect a growing trend toward multi-sectoral, policy-driven models that capture the structural complexity of labor markets.

In contemporary socio-economic research, mathematical modeling serves as a powerful paradigm to decipher the underlying complexities of population and labor dynamics. Unlike purely qualitative observations, mathematical frameworks formalize intricate feedback loops and evaluate long-term asymptotic behaviors. For instance, nonlinear differential equations are highly effective in capturing structural transitions and stability criteria within computational systems [14]. Furthermore, these models provide predictive power to simulate regime shifts, ensuring a deeper understanding of system sustainability under varied operational parameters [15], which can be validated through targeted methodological pipelines and empirical datasets [16]. Consequently, employing this mathematical framework transitions the analysis of the disability labor market from an observational perspective to a predictive, mechanism-based computational tool capable of informing long-term strategic governance.

Although many labor market models have been developed, several important research gaps remain in the existing literature. First, most frameworks rely on memoryless ordinary differential equations or statistical models that assume instantaneous transitions, thereby failing to represent institutional delays caused by workforce training, administrative procedures, and job matching. Second, existing theoretical delay models are rarely calibrated with empirical labor market data, which limits their direct policy interpretation. Third, current models often overlook seasonal vacancy patterns driven by recurrent annual policy interventions. To address these gaps, the main novelty of this study is the development of a nonlinear DDE framework explicitly tailored to Thailand's disability labor market. Unlike standard memoryless models, the proposed framework incorporates an implementation delay τ to represent operational time lags for persons with disabilities, and introduces a seasonal forcing term into the vacancy equation to capture policy-driven spikes. Under validation with Thailand's 2022–2025 quarterly statistics, this unified framework integrates delay-independent global stability analysis using Lyapunov functionals alongside a rigorous forward sensitivity framework to systematically evaluate system resilience and long-term equilibrium behavior.

The remainder of this paper is organized as follows. Section 2 presents the disability-unemployment model, which is represented by a nonlinear DDE. In Section 3, global asymptotic stability (GAS) using Lyapunov functionals and the LaSalle invariance principle is established. Next, parameter influence is examined through a forward sensitivity framework calibrated with empirical data in Section 4. Section 5 provides numerical validation of the theoretical results, and finally, Section 6 concludes with policy implications and future research directions.

2. The mathematical model

To analyze the dynamics of the disability labor market, let $U(t)$, $E(t)$, and $V(t)$ denote the number of unemployed persons with disabilities, employed persons with disabilities, and available vacancies reserved for persons with disabilities at time t, respectively. The model is developed based on the following assumptions:

(i) The number of unemployed persons with disabilities increases at a constant influx rate a_1, representing new entrants or newly registered persons. While this constant rate ensures mathematical tractability and stability analysis, it simplifies dynamic economic realities. For individuals with disabilities, empirical statistics show that their annual influx into the labor market remains relatively stable over time. However, a strictly constant rate may overlook sudden macroeconomic shocks or policy shifts. Therefore, investigating non-constant, time-varying, or state-dependent inflow rates represents a promising direction for future research to enhance model resilience.

(ii) The number of unemployed persons with disabilities may decrease due to migration or other factors at a rate proportional to their current number, denoted by $a_2U(t)$.

(iii) The transition from unemployment to employment occurs through two distinct pathways, namely, conventional recruitment, which is proportional to the matching between unemployed persons with disabilities and available vacancies at rate $a_3U(t)V(t)$, and public-sector assistance, where persons exit the unemployed persons with disabilities compartment at rate $a_4U(t)$ to undergo vocational training and subsequently enter the employed persons with disabilities compartment after a fixed policy implementation delay τ, represented by $a_4U(t-\tau)$. This specific delay explicitly models the mandatory timeframe under the Thai Persons with Disabilities Quality of Life Promotion Act (B.E. 2550). Under Sections 33–35, quota-related interventions (such as vocational training or internships) require structured durations for skills development and official registration, creating a policy-driven delay that dominates the transition process compared to conventional recruitment.

(iv) Employed persons with disabilities return to the unemployed persons with disabilities compartment due to layoffs at rate $b_1E(t)$, or exit the labor market permanently due to retirement at rate $b_2E(t)$.

(v) New vacancies for persons with disabilities are generated from two sources, consisting of vacancy replacement from a fraction of retirements at rate $b_3E(t)$, and public-sector expansion, where new vacancies are created at rate $c_1U(t)$ to support the growing number of unemployed persons with disabilities.

(vi) Job vacancies may be closed or expire due to financial constraints or administrative factors at a rate proportional to the existing vacancies, denoted by $c_2V(t)$.

The dynamic interactions described in these assumptions are illustrated in the schematic diagram shown in Figure 1.

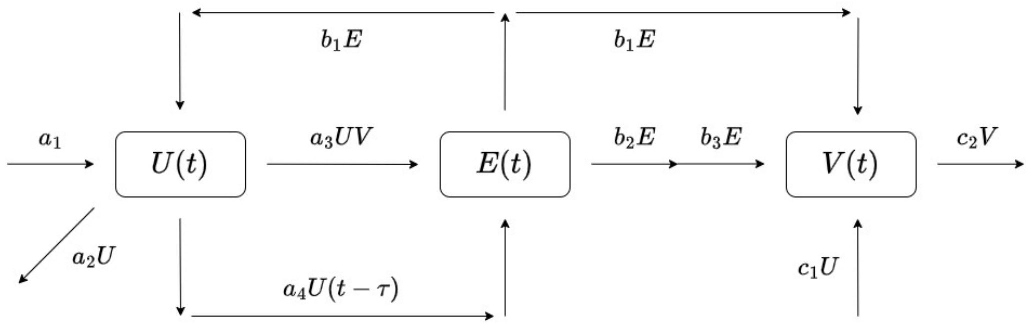

Figure 1. Schematic diagram of the disability labor market model (2.1) with policy delay τ.

The model structure and its associated parameters are summarized in Figure 1 and Table 1. Accordingly, the proposed model is represented by system (2.1):

$$
\begin{aligned}
\frac{dU(t)}{dt} &= a_1 - a_2U(t) - a_3U(t)V(t) - a_4U(t) + b_1E(t),\\
\frac{dE(t)}{dt} &= a_3U(t)V(t) + a_4U(t-\tau) - (b_1 + b_2)E(t),\\
\frac{dV(t)}{dt} &= (b_1 + b_3)E(t) + c_1U(t) - c_2V(t).
\end{aligned} \tag{2.1}
$$

The initial conditions and history functions for system (2.1) are assumed to be of the forms:

$$
\begin{aligned}
&U(\theta) = \phi_1(\theta), \quad E(\theta) = \phi_2(\theta), \quad V(\theta) = \phi_3(\theta),\\
&\phi_1(\theta) \geq 0, \quad \phi_2(\theta) \geq 0, \quad \phi_3(\theta) \geq 0, \quad \theta \in [-\tau, 0],\\
&\phi_1(0) > 0, \quad \phi_2(0) > 0, \quad \phi_3(0) > 0,
\end{aligned}
$$

where $\boldsymbol{\phi} = (\phi_1, \phi_2, \phi_3) \in C([-\tau, 0], \mathbb{R}^3_+)$.

The descriptions of the parameters used in system (2.1) are provided in Table 1. Note that all model parameters are assumed to be positive throughout this study.

Table 1. Parameters of the disability labor market model.

Param.	Explanation	Param.	Explanation
a_1	Constant influx of unemployed persons with disabilities into the market	b_2	Rate of retirement and permanent market exit
a_2	Migration rate of unemployed persons with disabilities	b_3	Vacancy replacement rate from retirement
a_3	Rate at which unemployed persons with disabilities become employed	c_1	Job creation rate for persons with disabilities
a_4	Implementation rate of government employment support for persons with disabilities	c_2	Job vacancy closure rate
b_1	Layoff rate	τ	Policy implementation delay

3. Dynamic analysis and stability

In this section, we analyze the system dynamics of model (2.1) to determine the stability properties. By using stability theory and linearization methods [17, 18], we examine the long-term dynamics of the system. Initially, to ensure the mathematical well-posedness of the model, we establish the non-negativity and boundedness of its solutions within the framework of delay-differential equations [19, 20]. The following lemma defines an invariant region Ω, which is shown to be positively invariant and globally attracting.

Lemma 3.1 (Positivity and boundedness)**.** *For any initial function* $\boldsymbol{\phi} = (\phi_1, \phi_2, \phi_3)^T \in C([-\tau, 0], \mathbb{R}^3_+)$ *such that* $\phi_i(\theta) \geq 0$ *for all* $\theta \in [-\tau, 0]$*, the solution* $\mathbf{x}(t) = (U(t), E(t), V(t))^T$ *of system* (2.1) *remains non-negative for all* $t \geq 0$*. Then, the region*

$$\Omega = \left\{ (U, E, V) \in \mathbb{R}^3_+ \mid 0 \leq U + E \leq \frac{a_1}{d_1}, \quad 0 \leq V \leq \frac{d_2 a_1}{c_2 d_1} \right\}$$

is positively invariant and globally attracting with respect to system (2.1)*, where* $d_1 = \min(a_2, b_2)$ *and* $d_2 = \max\{b_1 + b_3, c_1\}$*.*

Proof. First, the non-negativity of the solutions is presented. Given the initial functions $\phi_i(\theta) \geq 0$ for $\theta \in [-\tau, 0]$, we examine the vector field along the boundaries of the non-negative region

$$\begin{aligned}
\left.\frac{dU(t)}{dt}\right|_{U(t)=0} &= a_1 + b_1 E(t) \geq 0, \\
\left.\frac{dE(t)}{dt}\right|_{E(t)=0} &= a_3 U(t) V(t) + a_4 U(t - \tau) \geq 0, \\
\left.\frac{dV(t)}{dt}\right|_{V(t)=0} &= (b_1 + b_3) E(t) + c_1 U(t) \geq 0.
\end{aligned}$$

Since the system's trajectory remains inside $\mathbb{R}^3_+$ due to the direction of the vector field at the boundaries, any solution initiated in the non-negative region will stay non-negative for all $t \geq 0$ [19]. Next, for the boundedness proof, let $N(t) = U(t) + E(t)$. By summing the first two equations of (2.1), we obtain

$$\frac{dN(t)}{dt} = a_1 - a_2U(t) - b_2E(t).$$

Let $d_1 = \min(a_2, b_2)$. Since $U(t), E(t) \geq 0$, we obtain

$$\frac{dN(t)}{dt} \leq a_1 - d_1(U(t) + E(t)) = a_1 - d_1N(t).$$

By using the comparison principle [21], we obtain

$$N(t) \leq \frac{a_1}{d_1} + \left(N(0) - \frac{a_1}{d_1}\right)e^{-d_1t}.$$

By taking the limit supremum as $t \to \infty$, we obtain

$$\limsup_{t\to\infty} N(t) \leq \frac{a_1}{d_1}. \tag{3.1}$$

Now, consider the third equation of system (2.1):

$$\frac{dV(t)}{dt} = (b_1 + b_3)E(t) + c_1U(t) - c_2V(t).$$

Let $d_2 = \max\{b_1 + b_3, c_1\}$. By using (3.1), we obtain

$$\frac{dV(t)}{dt} \leq d_2(U(t) + E(t)) - c_2V(t) = d_2N(t) - c_2V(t).$$

According to (3.1), for any $\epsilon > 0$, there exists $T > 0$ such that $N(t) \leq \frac{a_1}{d_1} + \epsilon$ for all $t \geq T$. Consequently, we obtain

$$\frac{dV(t)}{dt} \leq d_2\left(\frac{a_1}{d_1} + \epsilon\right) - c_2V(t).$$

By applying the comparison principle again, we obtain

$$\limsup_{t\to\infty} V(t) \leq \frac{d_2a_1}{c_2d_1}. \tag{3.2}$$

Therefore, all solutions of system (2.1) are bounded and remain within the region Ω. Hence, Ω is positively invariant and globally attracting. □

3.1. Equilibrium points

Next, the existence of equilibrium points for system (2.1) is investigated.

Theorem 3.2. *Consider system* (2.1). *Define the parameters:*

$$\begin{aligned}
\alpha &= a_3[b_2c_1 - a_2(b_1 + b_3)],\\
\beta &= a_1a_3(b_1 + b_3) + a_2c_2(b_1 + b_2) + a_4b_2c_2,\\
\gamma &= a_1c_2(b_1 + b_2).
\end{aligned}$$

The positive equilibrium point $E_p(U^*, E^*, V^*)$ is determined by the positive root of the quadratic equation $\alpha(U^*)^2 + \beta U^* - \gamma = 0$. Furthermore, define

$$\delta(U^*) = a_1 - a_2 U^*,$$
$$\epsilon(U^*) = [b_2 c_1 - a_2(b_1 + b_3)]U^* + a_1(b_1 + b_3).$$

System (2.1) *has the following properties:*

(i) A unique positive equilibrium $E_{p1}(U_1, E_1, V_1)$ exists if $\alpha > 0$, where

$$U_1 = \frac{-\beta + \sqrt{\beta^2 + 4\alpha\gamma}}{2\alpha},$$

satisfying $U_1 > 0$ with the conditions $\delta(U_1) > 0$ and $\epsilon(U_1) > 0$.

(ii) At most two positive equilibria, $E_{p1}(U_1, E_1, V_1)$ and $E_{p2}(U_2, E_2, V_2)$, exist if $\alpha < 0$, provided $\beta^2 + 4\alpha\gamma > 0$, where

$$U_{1,2} = \frac{-\beta \pm \sqrt{\beta^2 + 4\alpha\gamma}}{2\alpha},$$

satisfying $U_{1,2} > 0$ with the conditions $\delta(U_l) > 0$ and $\epsilon(U_l) > 0$ for $l = 1, 2$.

(iii) A unique positive equilibrium $E_{p3}(U_3, E_3, V_3)$ exists if $\alpha = 0$, where

$$U_3 = \frac{\gamma}{\beta},$$

satisfying $U_3 > 0$ with the conditions $\delta(U_3) > 0$ and $\epsilon(U_3) > 0$.

In all cases, the components are given by:

$$E^* = \frac{\delta(U^*)}{b_2},$$
$$V^* = \frac{\epsilon(U^*)}{b_2 c_2}.$$

These strict positivity thresholds ensure that all structural equilibrium states remain non-negative, bounded, and economically meaningful within the invariant region Ω.

Proof. Let $E_{pl}(U^*, E^*, V^*)$ for $l \in \{1, 2, 3\}$ be an equilibrium point of system (2.1). By setting the right-hand side of (2.1) to zero, we obtain the following system of algebraic equations:

$$a_1 - a_2 U^* - a_3 U^* V^* - a_4 U^* + b_1 E^* = 0, \tag{3.3}$$
$$a_3 U^* V^* + a_4 U^* - b_1 E^* - b_2 E^* = 0, \tag{3.4}$$
$$b_1 E^* + b_3 E^* + c_1 U^* - c_2 V^* = 0. \tag{3.5}$$

By summing (3.3) and (3.4), we obtain

$$a_1 - a_2 U^* - b_2 E^* = 0.$$

By solving the above equation, we obtain

$$E^* = \frac{a_1 - a_2 U^*}{b_2} = \frac{\delta(U^*)}{b_2}. \tag{3.6}$$

By substituting (3.6) into (3.5) and solving, we obtain

$$\begin{aligned} c_2 V^* &= (b_1 + b_3)E^* + c_1 U^* = (b_1 + b_3)\left(\frac{a_1 - a_2 U^*}{b_2}\right) + c_1 U^*, \\ V^* &= \frac{[b_2 c_1 - a_2(b_1 + b_3)]U^* + a_1(b_1 + b_3)}{b_2 c_2}. \end{aligned}$$

Thus,

$$V^* = \frac{[b_2 c_1 - a_2(b_1 + b_3)]U^* + a_1(b_1 + b_3)}{b_2 c_2} = \frac{\epsilon(U^*)}{b_2 c_2}. \tag{3.7}$$

By substituting (3.6) and (3.7) back into (3.4), we obtain

$$\alpha(U^*)^2 + \beta U^* - \gamma = 0, \tag{3.8}$$

where α, β, γ are defined as in the statement of the theorem. The positive roots of the quadratic equation (3.8) determine the possible positive values of U^*. The existence of E_p depends on the algebraic sign of α and the existence conditions ($E^* > 0$ and $V^* > 0$), which are equivalent to the requirements $\delta(U^*) > 0$ and $\epsilon(U^*) > 0$. The details for Cases (i)–(iii) follow directly from the properties of the quadratic formula and these existence requirements. □

Remark 1. *The existence of the multiple equilibria state ($\alpha < 0$) occurs when $b_2 c_1 < a_2(b_1 + b_3)$, a condition representing a market with insufficient structural job creation. In this case, the rate of job expansion and vacancies arising from retirement fail to offset the cumulative effects of layoffs and labor market exits. Therefore, as this state reflects a structural failure rather than a desired policy objective, it is generally excluded from the operational focus of effective labor governance.*

3.2. Local stability analysis

To examine the local stability of the equilibrium points $E_l(U_l, E_l, V_l)$, defined in Theorem 3.2, we use linearization. We consider small perturbations $\mathbf{z}(t) = [\bar{u}(t), \bar{e}(t), \bar{v}(t)]^\top$ around the equilibrium point E_l. By substituting $\mathbf{x}(t) = E_l + \mathbf{z}(t)$ into system (2.1), we obtain

$$\mathbf{z}' = L_{1l}\mathbf{z}(t) + L_{2l}\mathbf{z}(t - \tau), \tag{3.9}$$

where L_{1l} and L_{2l} are the Jacobian matrices of the system evaluated at E_l:

$$L_{1l} = \begin{bmatrix} -(a_2 + a_4 + a_3 V_l) & b_1 & -a_3 U_l \\ a_3 V_l & -(b_1 + b_2) & a_3 U_l \\ c_1 & b_1 + b_3 & -c_2 \end{bmatrix} \quad \text{and} \quad L_{2l} = \begin{bmatrix} 0 & 0 & 0 \\ a_4 & 0 & 0 \\ 0 & 0 & 0 \end{bmatrix}.$$

The characteristic equation for the linearized system (3.9) is given by the determinant $\det(\lambda I - L_{1l} - L_{2l}e^{-\lambda\tau}) = 0$. After algebraic expansion, we obtain

$$\lambda^3 + p_{1l}\lambda^2 + p_{2l}\lambda + p_{3l} + (q_{1l}\lambda + q_{2l})e^{-\lambda\tau} = 0, \tag{3.10}$$

where

$$
\begin{aligned}
p_{1l} &= (a_2 + a_4 + a_3 V_l) + (b_1 + b_2) + c_2,\\
p_{2l} &= (a_2 + a_4)[(b_1 + b_2) + c_2] + c_2(b_1 + b_2) + a_3(b_2 + c_2)V_l + a_3[c_1 - (b_1 + b_3)]U_l,\\
p_{3l} &= c_2(a_2 + a_4)(b_1 + b_2) + a_3 b_2 c_2 V_l + a_3[b_2 c_1 - (a_2 + a_4)(b_1 + b_3)]U_l,\\
q_{1l} &= -a_4 b_1,\\
q_{2l} &= a_3 a_4 (b_1 + b_3)U_l - a_4 b_1 c_2.
\end{aligned}
$$

The equilibrium point E_l is locally asymptotically stable if all roots of (3.10) have negative real parts.

3.2.1. Stability analysis for $\tau = 0$

By setting $\tau = 0$ in the characteristic equation (3.10), we obtain

$$\lambda^3 + p_{1l}\lambda^2 + (p_{2l} + q_{1l})\lambda + (p_{3l} + q_{2l}) = 0. \tag{3.11}$$

The stability of E_l for $\tau = 0$ is determined by the Routh-Hurwitz criterion [22].

3.2.2. Stability analysis for $\tau > 0$

For $\tau > 0$, we investigate the existence of purely imaginary roots $\lambda = i\omega$ ($\omega > 0$) by separating the real and imaginary parts of (3.10). By squaring the separated real and imaginary parts, we obtain the required transcendental equation for $\sigma = \omega^2$:

$$\sigma^3 + c_{1l}\sigma^2 + c_{2l}\sigma + c_{3l} = 0, \tag{3.12}$$

where c_{1l}, c_{2l}, c_{3l} are the coefficients previously defined. The characteristic equation (3.10) has purely imaginary roots if and only if (3.12) has at least one positive real root. For simplication, we define

$$F_l(\sigma) = \sigma^3 + c_{1l}\sigma^2 + c_{2l}\sigma + c_{3l}.$$

Next, we analyze the polynomial (3.12) using the methodology for transcendental equations given by Ruan and Wei [23]. According to the work, the following lemma provides the condition for the absence of positive roots.

Lemma 3.3 (Ruan-Wei criterion)**.** *Suppose* $\sigma_{0l} = \frac{1}{3}(-c_{1l} + \sqrt{c_{1l}^2 - 3c_{2l}})$ *and the equilibrium point* E_l *exists. If one of the following holds:*

(i) $c_{3l} \geq 0$ *and* $c_{1l}^2 < 3c_{2l}$*;*
(ii) $c_{3l} \geq 0$ *and* $\sigma_{0l} \leq 0$*;*
(iii) $c_{3l} \geq 0$ *and* $\sigma_{0l} > 0$ *and* $F_l(\sigma_{0l}) > 0$*,*

then the polynomial $\sigma^3 + c_{1l}\sigma^2 + c_{2l}\sigma + c_{3l} = 0$ *has no positive roots.*

Therefore, if the conditions of Lemma 3.3 are satisfied, the system cannot have purely imaginary eigenvalues, and thus, a Hopf bifurcation cannot occur.

Simplification of coefficients. We first calculate the expression for $c_{3l} = p_{3l}^2 - q_{2l}^2 = (p_{3l} + q_{2l})(p_{3l} - q_{2l})$. By substituting the algebraic expressions for p_{3l} and q_{2l} and simplifying, we obtain

$$p_{3l} + q_{2l} = a_2c_2(b_1 + b_2) + a_4b_2c_2 + a_3[b_2c_1 - a_2(b_1 + b_3)]U_l + a_3b_2c_2V_l, \tag{3.13}$$

$$p_{3l} - q_{2l} = c_2(a_2 + a_4)(b_1 + b_2) + a_4b_1c_2 + a_3[b_2c_1 - (a_2 + 2a_4)(b_1 + b_3)]U_l + a_3b_2c_2V_l. \tag{3.14}$$

The stability of the equilibrium E_l for $\tau = 0$ is determined by applying the Routh-Hurwitz stability criterion [17, 22, 24] to the cubic polynomial (3.11).

Proposition 3.4 (Stability at $\tau = 0$)**.** *The equilibrium point E_l is locally asymptotically stable when $\tau = 0$ if and only if the coefficients of* (3.11) *satisfy the Routh-Hurwitz conditions:*

(i) the coefficients $P_1 = p_{1l} > 0$, $P_2 = p_{2l} + q_{1l} > 0$, and $P_3 = p_{3l} + q_{2l} > 0$;
(ii) $P_1P_2 > P_3$.

Based on the analysis of these coefficients, we establish the following propositions for delay-independent stability of the existing positive equilibrium points.

Remark 2. *The present study focuses on deriving sufficient conditions that guarantee delay-independent stability of the positive equilibrium. Consequently, the analysis is restricted to parameter regions in which the characteristic equation admits no purely imaginary roots. When the conditions of Lemma 3.3 are violated, purely imaginary roots may arise and the system may undergo a Hopf bifurcation, leading to periodic oscillations in unemployment, employment, and vacancy levels. A complete investigation of the existence, direction, and stability of Hopf bifurcations requires additional center manifold and normal form analysis, and is beyond the scope of the present work.*

Proposition 3.5 (Delay-independent stability for E_{p1})**.** *Assume the positive equilibrium E_{p1} exists ($\alpha > 0$). The equilibrium point E_{p1} is locally asymptotically stable for all $\tau \geq 0$ if the following conditions hold:*

(A) The coefficients $p_{31} + q_{21} > 0$ and $p_{31} - q_{21} > 0$, which ensures $c_{31} > 0$.
(B) One of the following holds for the polynomial $F_1(\sigma)$:
  (i) $c_{11}^2 < 3c_{21}$,
  (ii) $\sigma_{01} \leq 0$,
  (iii) $\sigma_{01} > 0$ and $F_1(\sigma_{01}) > 0$,

where σ_{01} is the positive local minimum of $F_1(\sigma)$.

Proof. The first set of conditions (A) ensures that $c_{31} > 0$. This, combined with conditions (B), guarantees by Lemma 3.3 that the characteristic equation (3.10) has no positive real roots for $\sigma = \omega^2$, and thus no purely imaginary roots for any $\tau \geq 0$. By Proposition 3.4, the equilibrium E_{p1} is stable at $\tau = 0$. Consequently, the stability is preserved for all $\tau \geq 0$. □

Proposition 3.6 (Delay-independent stability for E_{p3})**.** *Assume the positive equilibrium E_{p3} exists ($\alpha = 0$). The equilibrium point E_{p3} is locally asymptotically stable for all $\tau \geq 0$ if the following conditions hold:*

(A) The coefficients $p_{33} + q_{23} > 0$ and $p_{33} - q_{23} > 0$, which ensures $c_{33} > 0$.

(B) One of the following holds for the polynomial $F_3(\sigma)$:

(i) $c_{13}^2 < 3c_{23}$,
(ii) $\sigma_{03} \le 0$,
(iii) $\sigma_{03} > 0$ *and* $F_3(\sigma_{03}) > 0$,

where σ_{03} is the positive local minimum of $F_3(\sigma)$.

Proof. The proof is similar to the proof of Proposition 3.5, but applied to the coefficients c_{i3} and σ_{03} corresponding to the equilibrium E_{p3}. □

Based on the analysis of (3.10) and the criteria established in Lemma 3.3 and Propositions 3.4–3.6, we now summarize the local asymptotic stability conditions for the positive equilibrium points E_{p1} and E_{p3} in the following theorems.

Theorem 3.7. *Assume that the positive equilibrium E_{p1} exists ($\alpha > 0$, $\delta_1 > 0$, and $\epsilon_1 > 0$). If the following conditions are satisfied:*

(i) $c_1 \ge b_1 + b_3$, $b_2c_1 \ge (a_2 + 2a_4)(b_1 + b_3)$, $a_2 \ge b_2$,
(ii) one of the conditions in Proposition 3.5 (B) holds,

then E_{p1} is locally asymptotically stable for all $\tau \ge 0$.

Proof. The local asymptotic stability of E_{p1} for all $\tau \ge 0$ is established in two steps:

- For $\tau = 0$, the characteristic equation (3.11) has roots with negative real parts, as verified by Proposition 3.4 under the specified parameter conditions.
- For $\tau > 0$, the absence of purely imaginary roots ($\lambda = i\omega$) is guaranteed by Proposition 3.5, ensuring that no stability switch or Hopf bifurcation occurs.

Since the equilibrium is stable at $\tau = 0$ and no stability switch occurs for $\tau > 0$, the stability is preserved for all $\tau \ge 0$. □

Theorem 3.8. *Assume that the positive equilibrium E_{p3} exists ($\alpha = 0, \delta_3 > 0$, and $\epsilon_3 > 0$). If the following conditions are satisfied:*

(i) $c_1 \ge b_1 + b_3$ *and* $b_2c_1 \ge 2a_4(b_1 + b_3)$,
(ii) one of the conditions in Proposition 3.6 (B) holds,

then E_{p3} is locally asymptotically stable for all $\tau \ge 0$.

Proof. The local asymptotic stability of E_{p3} for all $\tau \ge 0$ is established in two steps:

- For $\tau = 0$, the characteristic equation (3.11) has roots with negative real parts, as verified by Proposition 3.4 under the specified parameter conditions.
- For $\tau > 0$, the absence of purely imaginary roots ($\lambda = i\omega$) is guaranteed by Proposition 3.6, ensuring that no stability switch or Hopf bifurcation occurs.

Since the equilibrium is stable at $\tau = 0$ and no stability switch occurs for $\tau > 0$, the stability is preserved for all $\tau \ge 0$. □

3.3. Global stability analysis

Further, we investigate the GAS of system (2.1) using the Lyapunov functional method and the LaSalle invariance principle [17, 20, 25]. We first define a Lyapunov functional as follows:

$$W_l(t) = U_l g\left(\frac{U}{U_l}\right) + E_l g\left(\frac{E}{E_l}\right) + V_l g\left(\frac{V}{V_l}\right) + a_4 U_l \int_{t-\tau}^{t} g\left(\frac{U(s)}{U_l}\right) ds,$$

where $l = 1, 3$ and the function $g(y) = y - 1 - \ln(y)$. Note that $W_l(t) \geq 0$ for all positive U, E, V, and the global minimum $W_l(t) = 0$ occurs at E_{pl}. We establish the global stability conditions in the following theorems.

Theorem 3.9. *Assume that the positive equilibrium E_{p1} exists ($\alpha > 0, \delta_1 > 0$, and $\epsilon_1 > 0$). If the following conditions are satisfied:*

(A) $a_2 \geq c_1$, $b_2 \geq b_1 + b_3$, and $c_2 \geq a_3 U_1$,
(B) the local stability conditions of E_{p1} hold,

then E_{p1} is globally asymptotically stable (GAS) for all $\tau \geq 0$.

Proof. Define a Lyapunov functional $W_1(t)$. By differentiating $W_1(t)$ along the solutions of system (2.1), it can be shown that the derivative is given by

$$\begin{aligned}\frac{dW_1}{dt} &= (c_1 - a_2)U_1 g\left(\frac{U}{U_1}\right) - a_1 g\left(\frac{U_1}{U}\right) + (b_1 + b_3 - b_2)E_1 g\left(\frac{E}{E_1}\right) \\ &+ (a_3 U_1 - c_2)V_1 g\left(\frac{V}{V_1}\right) - b_1 E_1 g\left(\frac{U_1 E}{U E_1}\right) - a_4 U_1 g\left(\frac{E_1 U(t-\tau)}{E U_1}\right) \\ &- a_3 U_1 V_1 g\left(\frac{E_1 U V}{E U_1 V_1}\right) - c_1 U_1 g\left(\frac{V_1 U}{V U_1}\right) - (b_1 + b_3)E_1 g\left(\frac{V_1 E}{V E_1}\right).\end{aligned}$$

Under condition (A), where $a_2 \geq c_1$, $b_2 \geq b_1 + b_3$, and $c_2 \geq a_3 U_1$, it follows that $dW_1/dt \leq 0$ since $g(y) \geq 0$ for all $y > 0$. The equality $dW_1/dt = 0$ holds if and only if $U(t) = U(t-\tau) = U_1$, $E = E_1$, and $V = V_1$. By the LaSalle invariance principle [25], the solution converges to the largest invariant set, which is the equilibrium E_{p1}. Furthermore, since the local stability is ensured by condition (B), we conclude that E_{p1} is GAS for all $\tau \geq 0$. For the complete, step-by-step algebraic expansion of the Lyapunov derivative and verification details, please refer to Appendix A. □

Theorem 3.10. *Assume that the positive equilibrium E_{p3} exists ($\alpha = 0, \delta_3 > 0$, and $\epsilon_3 > 0$). If the following conditions are satisfied:*

(A) $a_2 \geq c_1$, $b_2 \geq b_1 + b_3$, and $c_2 \geq a_3 U_3$,
(B) the local stability conditions of E_{p3} hold,

then E_{p3} is GAS for all $\tau \geq 0$.

Proof. The proof is similar to that of Theorem 3.9. By differentiating the Lyapunov functional $W_3(t)$ along the solutions of system (2.1), it follows from condition (A) that $dW_3/dt \leq 0$. The equality $dW_3/dt = 0$ holds if and only if the solution is at the equilibrium E_{p3}. By the LaSalle invariance principle [25], the solution converges to the largest invariant set, which is E_{p3}. Furthermore, since the local stability is ensured by condition (B), we conclude that E_{p3} is GAS for all $\tau \geq 0$. The exhaustive mathematical tracking and detailed transitions are provided in Appendix B. □

4. Parameter estimation and forward sensitivity analysis

This section bridges the theoretical stability analysis with a data-driven evaluation of the model. The primary objective is to assess the robustness of the model's predictions and to identify the parameters that most strongly influence system dynamics. In particular, model parameters are first estimated using Thai labor statistics from 2022–2025. Subsequently, a forward sensitivity analysis is conducted to compute the normalized sensitivity indices (SI). This analysis enables the identification of key parameters that govern employment dynamics and system stability, thereby providing a quantitative foundation for the policy recommendations presented in the subsequent sections.

4.1. Parameter estimation based on statistical data

In accordance with the methodological framework proposed by Arriola and Hyman [26], the parameter estimation process is formulated as a functional mapping $\mathcal{F} : \mathcal{SD} \to \Omega_P$, where $\mathcal{SD}$ denotes the statistical dataset and Ω_P represents the parameter space. Specifically, parameter estimation is performed using the Nelder-Mead simplex algorithm within a numerical computing environment, while the system trajectories are evaluated using a delay-differential equation solver. The objective function minimizes the sum of squared residuals (SSR) between Thailand's observed quarterly labor market data and the model predictions over a 16-quarter period. To ensure both mathematical and practical consistency, a penalty-function approach is employed to enforce parameter constraints and ensure that the estimated parameters satisfy the global stability conditions established in Theorem 3.9. The optimization procedure terminates when the convergence criteria are met, with the function tolerance and step-size tolerance set to 10^{-12} and 10^{-10}, respectively.

We define the global parameter vector as

$$\mathbf{p} = \{a_1, a_2, a_3, a_4, b_1, b_2, b_3, c_1, c_2\} \in \mathbb{R}^9_+. \tag{4.1}$$

The parameter values are determined to ensure that the model accurately reflects the structural characteristics of the Thai disability labor market. In particular, parameters associated with labor inflow and attrition rates, $\{a_1, a_2, a_4, b_1, b_2\}$, are directly inferred from statistical data provided by the Department of Empowerment of Persons with Disabilities [27] and the National Statistical Office [28].

The remaining parameters, $\{a_3, b_3, c_1, c_2\}$, are calibrated to align the model outputs with observed longitudinal trends. Specifically, these parameters are estimated so that the system converges to the positive equilibrium $E_{p1} \approx [737761, 67589, 32843]^\top$, which is used as the baseline reference state for subsequent analysis.

4.2. Mathematical derivation of the forward sensitivity system

To provide a rigorous mathematical foundation for the sensitivity analysis, we examine the response of the equilibrium point U^* to small perturbations in the parameter vector $\mathbf{p}$.

Based on Case (i) of Theorem 3.2, which corresponds to the observed disability labor market, the equilibrium U^* satisfies the quadratic equation

$$\alpha(U^*)^2 + \beta U^* - \gamma = 0, \tag{4.2}$$

where α, β, and γ depend on the parameter vector $\mathbf{p}$.

Differentiating (4.2) implicitly with respect to any parameter $p \in \mathbf{p}$ yields

$$\frac{\partial \alpha}{\partial p}(U^*)^2 + 2\alpha U^* \frac{\partial U^*}{\partial p} + \frac{\partial \beta}{\partial p} U^* + \beta \frac{\partial U^*}{\partial p} - \frac{\partial \gamma}{\partial p} = 0. \tag{4.3}$$

Solving for $\frac{\partial U^*}{\partial p}$, we obtain

$$\frac{\partial U^*}{\partial p} = \frac{\dfrac{\partial \gamma}{\partial p} - U^* \dfrac{\partial \beta}{\partial p} - (U^*)^2 \dfrac{\partial \alpha}{\partial p}}{2\alpha U^* + \beta}. \tag{4.4}$$

Under the conditions of Case (i) in Theorem 3.2, the denominator satisfies $2\alpha U^* + \beta = \sqrt{\Delta}$, where $\Delta = \beta^2 + 4\alpha\gamma$ is the discriminant of (4.2). Consequently, the sensitivity expression simplifies to

$$\frac{\partial U^*}{\partial p} = \frac{1}{\sqrt{\Delta}} \left(\frac{\partial \gamma}{\partial p} - U^* \frac{\partial \beta}{\partial p} - (U^*)^2 \frac{\partial \alpha}{\partial p} \right). \tag{4.5}$$

The normalized sensitivity index (SI), denoted by $S_{U,p}$, quantifies the relative impact of parameter variations on the equilibrium point [29] and is defined as

$$S_{U,p} = \left(\frac{\partial U^*}{\partial p} \right) \left(\frac{p}{U^*} \right), \tag{4.6}$$

where U^* corresponds to the equilibrium obtained in Case (i) of Theorem 3.2.

To provide a detailed description of the numerical analysis, the explicit analytical forms of the sensitivity gradients for each parameter $p \in \mathbf{p}$ are presented below. These expressions are derived by substituting the partial derivatives of the structural coefficients $\alpha, \beta,$ and γ into the implicit differentiation framework established in (4.5).

(i) Constant influx of unemployed persons with disabilities (a_1):

$$\frac{\partial U^*}{\partial a_1} = \frac{1}{\sqrt{\Delta}} \left[c_2(b_1 + b_2) - U^* a_3(b_1 + b_3) \right], \tag{4.7}$$

$$S_{U,a_1} = \frac{\partial U^*}{\partial a_1} \cdot \frac{a_1}{U^*}. \tag{4.8}$$

(ii) Migration rate of the unemployed disability population (a_2):

$$\frac{\partial U^*}{\partial a_2} = \frac{1}{\sqrt{\Delta}} \left[-U^* c_2(b_1 + b_2) + (U^*)^2 a_3(b_1 + b_3) \right], \tag{4.9}$$

$$S_{U,a_2} = \frac{\partial U^*}{\partial a_2} \cdot \frac{a_2}{U^*}. \tag{4.10}$$

(iii) Rate of transition from unemployment to employment (a_3):

$$\frac{\partial U^*}{\partial a_3} = \frac{1}{\sqrt{\Delta}} \left[-U^* a_1(b_1 + b_3) - (U^*)^2 (b_2 c_1 - a_2(b_1 + b_3)) \right], \tag{4.11}$$

$$S_{U,a_3} = \frac{\partial U^*}{\partial a_3} \cdot \frac{a_3}{U^*}. \tag{4.12}$$

(iv) Implementation rate of state employment support policies (a_4):

$$\frac{\partial U^*}{\partial a_4} = \frac{1}{\sqrt{\Delta}} \left[-U^* b_2 c_2\right], \tag{4.13}$$

$$S_{U,a_4} = \frac{\partial U^*}{\partial a_4} \cdot \frac{a_4}{U^*}. \tag{4.14}$$

(v) Layoff and separation rate (b_1):

$$\frac{\partial U^*}{\partial b_1} = \frac{1}{\sqrt{\Delta}} \left[a_1 c_2 - U^*(a_1 a_3 + a_2 c_2) + (U^*)^2 a_2 a_3\right], \tag{4.15}$$

$$S_{U,b_1} = \frac{\partial U^*}{\partial b_1} \cdot \frac{b_1}{U^*}. \tag{4.16}$$

(vi) Rate of retirement and permanent labor market exit (b_2):

$$\frac{\partial U^*}{\partial b_2} = \frac{1}{\sqrt{\Delta}} \left[a_1 c_2 - U^*(a_2 c_2 + a_4 c_2) - (U^*)^2 a_3 c_1\right], \tag{4.17}$$

$$S_{U,b_2} = \frac{\partial U^*}{\partial b_2} \cdot \frac{b_2}{U^*}. \tag{4.18}$$

(vii) Vacancy replacement rate following retirement (b_3):

$$\frac{\partial U^*}{\partial b_3} = \frac{1}{\sqrt{\Delta}} \left[-U^* a_1 a_3 + (U^*)^2 a_2 a_3\right], \tag{4.19}$$

$$S_{U,b_3} = \frac{\partial U^*}{\partial b_3} \cdot \frac{b_3}{U^*}. \tag{4.20}$$

(viii) Job creation rate for persons with disabilities (c_1):

$$\frac{\partial U^*}{\partial c_1} = \frac{1}{\sqrt{\Delta}} \left[-(U^*)^2 a_3 b_2\right], \tag{4.21}$$

$$S_{U,c_1} = \frac{\partial U^*}{\partial c_1} \cdot \frac{c_1}{U^*}. \tag{4.22}$$

(ix) Job vacancy closure and attrition rate (c_2):

$$\frac{\partial U^*}{\partial c_2} = \frac{1}{\sqrt{\Delta}} \left[a_1(b_1 + b_2) - U^*(a_2(b_1 + b_2) + a_4 b_2)\right], \tag{4.23}$$

$$S_{U,c_2} = \frac{\partial U^*}{\partial c_2} \cdot \frac{c_2}{U^*}. \tag{4.24}$$

The explicit gradients (4.7)–(4.23) provide a comprehensive mapping of how parameter perturbations impact the equilibrium stability of the disability labor market. This analytical framework ensures that the numerical sensitivities reported in Table 7 are derived from the underlying nonlinear dynamics proven in Theorem 3.2.

5. Numerical simulation and discussion

In this section, numerical simulations are presented to validate the theoretical results from the preceding sections. The experiments are organized into three parts. First, synthetic parameter values are used to verify the stability conditions and to investigate the influence of different delay values τ on transient system behavior over the simulation interval $t \in [0, 1000]$. Second, the model is calibrated and applied to Thailand's disability labor market using empirical quarterly data from 2022–2025, where a seasonal forcing term is incorporated into the vacancy equation to reproduce the observed periodic vacancy spikes. Finally, a sensitivity analysis is performed to evaluate the influence of individual parameters on the equilibrium and identify the key factors affecting long-term system behavior. Numerical solutions of the DDE system are obtained using an explicit Runge–Kutta $(2, 3)$ pair with adaptive step-size control, relative tolerance 10^{-3}, and absolute tolerance 10^{-6}. Since the solver employs adaptive time-stepping, no fixed step size is prescribed. The parameter values used in each experiment are listed in the corresponding parameter tables, while the values of the varying parameters are specified in the associated figure captions and discussion.

5.1. Theoretical validation of stability criteria

In this subsection, we verify the stability criteria using simulated parameter values to demonstrate the consistency of Theorems 3.9 and 3.10. This initial validation ensures that the numerical simulations of the model coincide with the analytical results derived in Section 3 before proceeding to case study applications.

5.1.1. Global stability of E_{p1} and E_{p3}

In this subsection, we present the results of numerical experiments to verify the GAS of the system under the first case. To demonstrate global stability, three sets of initial conditions, denoted as

$$\mathbf{x}_0^i = [U_0^i, E_0^i, V_0^i]^\top$$

for $i = 1, 2, 3$, are chosen as follows:

$$\mathbf{x}_0^1 = \begin{bmatrix} 80,000 \\ 10,000 \\ 8,000 \end{bmatrix}, \mathbf{x}_0^2 = \begin{bmatrix} 10,000 \\ 50,000 \\ 3,000 \end{bmatrix}, \quad \text{and} \quad \mathbf{x}_0^3 = \begin{bmatrix} 90,000 \\ 60,000 \\ 9,000 \end{bmatrix}.$$

The simulated parameter values are chosen to satisfy the conditions of Theorem 3.9, as summarized in Table 2.

Table 2. Parameter values satisfying conditions for Theorem 3.9 (E_{p1}).

Parameters	Values	Parameters	Values
a_1	5,000	b_2	0.05
a_2	0.1	b_3	0.01
a_3	4×10^{-6}	c_1	0.08
a_4	0.01	c_2	0.72
b_1	0.01		

Similarly, we present the results of numerical experiments that verify the GA stability of the system for the boundary case E_{p3}. To demonstrate global stability, three sets of initial conditions are chosen as follows:

$$\mathbf{x}_0^1 = \begin{bmatrix} 80,000 \\ 10,000 \\ 15,000 \end{bmatrix}, \quad \mathbf{x}_0^2 = \begin{bmatrix} 10,000 \\ 40,000 \\ 5,000 \end{bmatrix}, \quad \text{and} \quad \mathbf{x}_0^3 = \begin{bmatrix} 70,000 \\ 5,000 \\ 10,000 \end{bmatrix}.$$

The simulated parameter values are chosen to satisfy the conditions of Theorem 3.10, as summarized in Table 3.

Table 3. Parameter values satisfying conditions for Theorem 3.10 (E_{p3}).

Parameters	Values	Parameters	Values
a_1	3,500	b_2	0.04
a_2	0.05	b_3	0.02
a_3	1×10^{-6}	c_1	0.05
a_4	0.001	c_2	0.35
b_1	0.02		

The simulation results, shown in Figures 2 and 3, demonstrate that all trajectories converge to their equilibria,

$$E_{p1} \approx [40000, 20000, 5000]^\top$$

and

$$E_{p3} \approx [61046, 11191, 10000]^\top,$$

regardless of initial perturbations. This behavior confirms the presence of stable labor market behavior and validates the delay-independent global stability established in Section 3. In particular, Figure 2 verified the GA stability of E_{p1}. It can be seen that the system autonomously returns to equilibrium despite significant disturbances or organizational delays ($\tau = 10$), in agreement with Theorem 3.9. Similarly, Figure 3 confirms the GA stability of E_{p3}, demonstrating that the system maintains a stable long-term state even under highly imbalanced conditions, as stated in Theorem 3.10. These results show the robustness of the model and its ability to absorb structural imbalances and extreme shocks, ensuring sustained equilibrium without continuous external intervention.

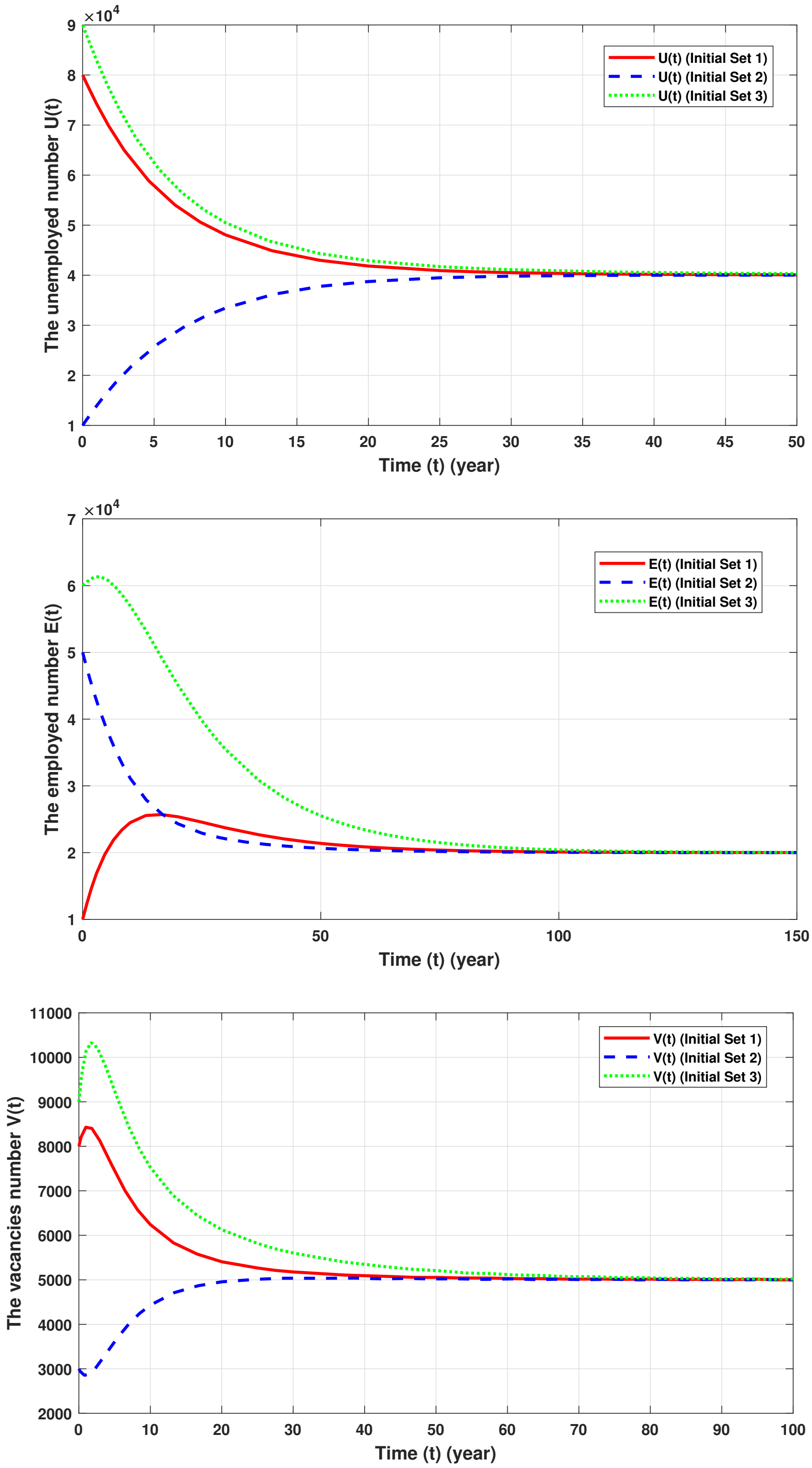

Figure 2. Global stability of E_{p1} under Theorem 3.9 with $\tau = 10$, demonstrating convergence from distinct initial conditions to the equilibrium (U_1, E_1, V_1) based on parameters in Table 2.

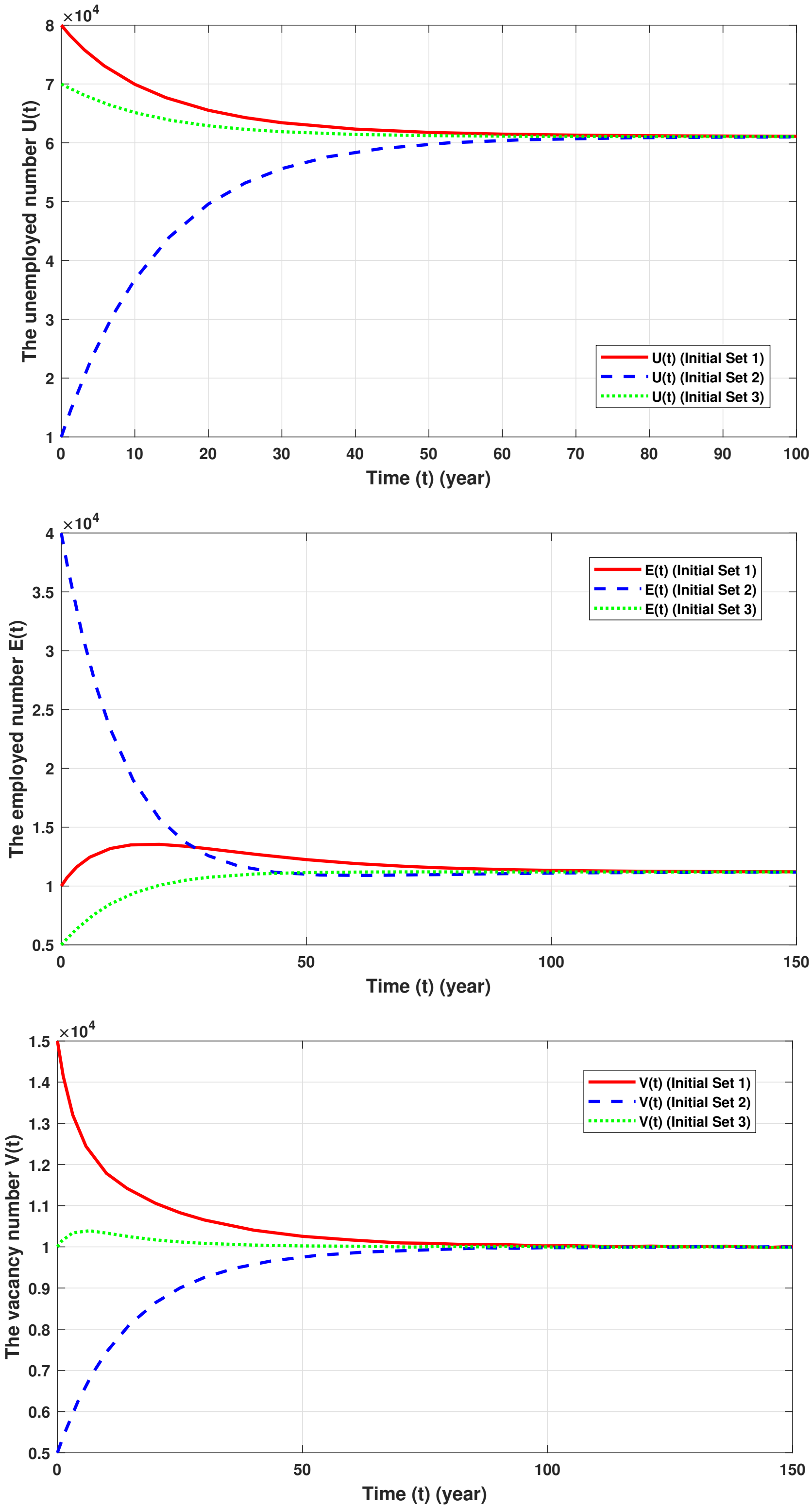

Figure 3. Global stability of E_{p3} under Theorem 3.10 with $\tau = 10$, demonstrating convergence from distinct initial conditions to the equilibrium (U_3, E_3, V_3) based on parameters in Table 3.

5.1.2. Impact of time delay τ and implementation rate a_4

In this subsection, we investigate the sensitivity of the system to variations in the time delay (τ) associated with the matching process and the implementation rate of government employment support (a_4). This analysis is essential for understanding how administrative delays and policy execution interact to influence system stability and convergence behavior.

We first examine the impact of the delay parameter τ on the stability of the equilibrium points E_{p1} and E_{p3}. To capture different levels of organizational and matching delays, three representative cases with varying delay magnitudes are considered, as detailed in Tables 2 and 3.

For the first case (E_{p1}, illustrated in Figure 4), the initial condition is given by

$$\mathbf{x}_0 = \begin{bmatrix} U(0) \\ E(0) \\ V(0) \end{bmatrix} = \begin{bmatrix} 80,000 \\ 10,000 \\ 8,000 \end{bmatrix}.$$

For the second case (E_{p3}, illustrated in Figure 5), the initial condition is

$$\mathbf{x}_0 = \begin{bmatrix} U(0) \\ E(0) \\ V(0) \end{bmatrix} = \begin{bmatrix} 80,000 \\ 10,000 \\ 15,000 \end{bmatrix}.$$

The simulation results (Figures 4 and 5) show that the system remains asymptotically stable for all considered values of the delay parameter τ. However, increasing τ significantly slows the convergence rate and induces more pronounced transient oscillations, reflecting temporary market imbalances during the adjustment process. In both cases, although global stability is preserved for all delay magnitudes ($\tau = 1, 10, 100$), larger delays act as a dynamic amplifier of market volatility. Specifically, shorter delays lead to a smooth and rapid return to equilibrium, whereas longer delays (particularly $\tau = 100$) produce high-amplitude oscillations that substantially prolong convergence. These findings suggest that, while organizational and policy implementation delays do not compromise long-term stability, they significantly reduce the efficiency of the adjustment process and extend the duration of structural imbalances in the labor market.

Next, we investigate the effect of the implementation rate a_4 on the unemployed population $U(t)$. To evaluate the effectiveness of government-funded assistive programs, three scenarios with different values of a_4 are considered, as summarized in Table 4. The initial condition for this experiment is given by

$$\mathbf{x}_0 = \begin{bmatrix} U(0) \\ E(0) \\ V(0) \end{bmatrix} = \begin{bmatrix} 50,000 \\ 20,000 \\ 5,000 \end{bmatrix}.$$

Table 4. Parameter values for analyzing the impact of a_4 variation.

Parameters	**Set 1**	**Set 2**	**Set 3**
a_4	0.010	0.025	0.050
Other parameters	Consistent with Table 2		

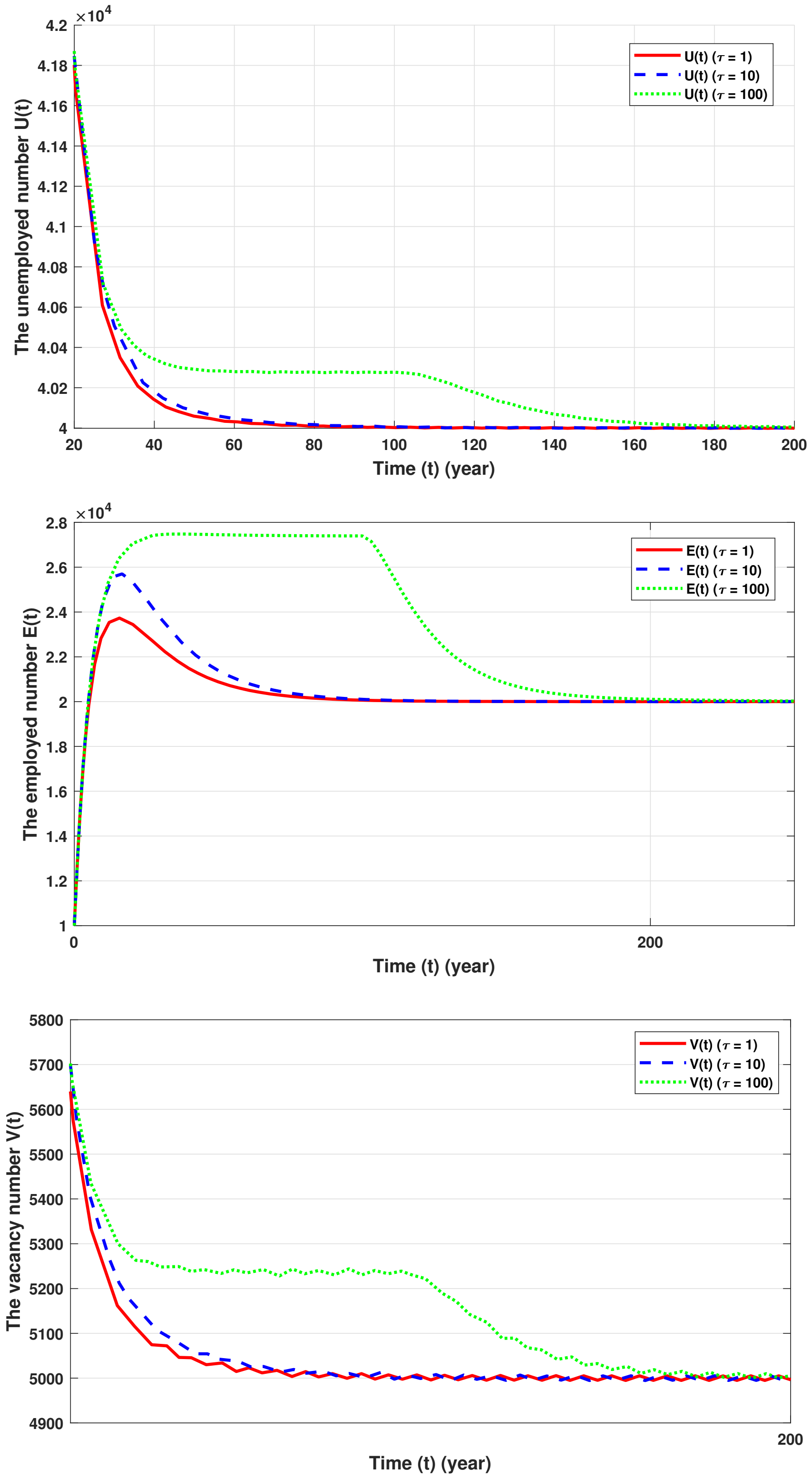

Figure 4. Global stability of E_{p1} under Theorem 3.9 for $\tau \in \{1, 10, 100\}$, demonstrating delay-independent convergence to the equilibrium (U_1, E_1, V_1) based on parameters in Table 2.

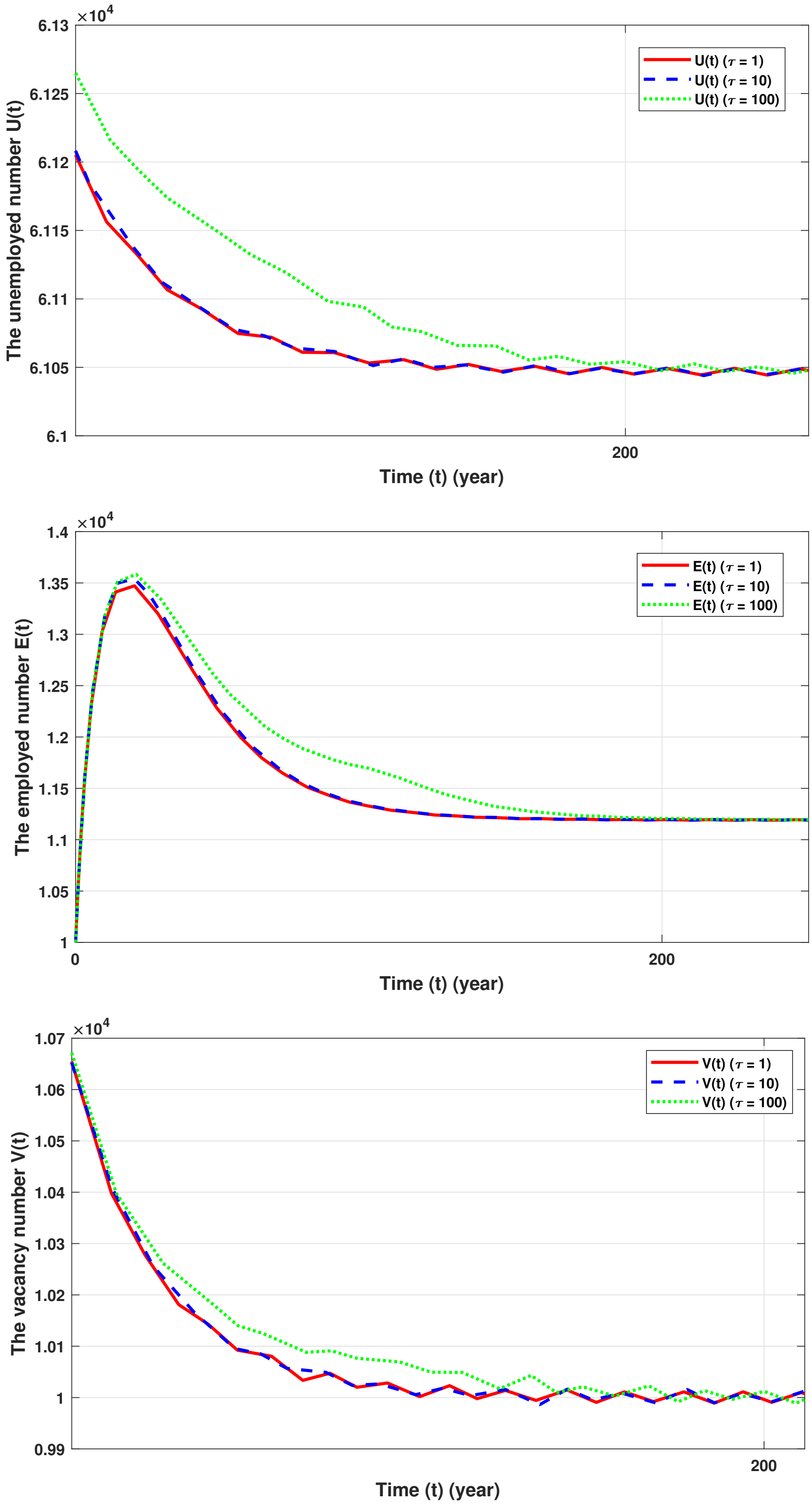

Figure 5. Global stability of E_{p3} under Theorem 3.10 for $\tau \in \{1, 10, 100\}$, demonstrating delay-independent convergence to the equilibrium (U_3, E_3, V_3) based on parameters in Table 3.

As shown in Figure 6, increasing the government implementation rate (a_4) leads to a reduction in the long-term unemployment level U^*. This observation is consistent with the normalized sensitivity index $S_{U,a_4} = -0.03597570$ reported in Section 5.3. It confirms that enhanced job placement policies effectively reduce unemployment persistence and improve system recovery. From a systemic perspective, a_4 serves as a key policy lever for promoting inclusive employment among persons with disabilities. However, the presence of implementation delays ($\tau = 10$) induces transient oscillations and prolongs the adjustment period. It is seen that increasing a_4 helps reduce unemployment in the long run, but delays in implementation can cause short-term fluctuations and slow down the system's progress toward a stable state.

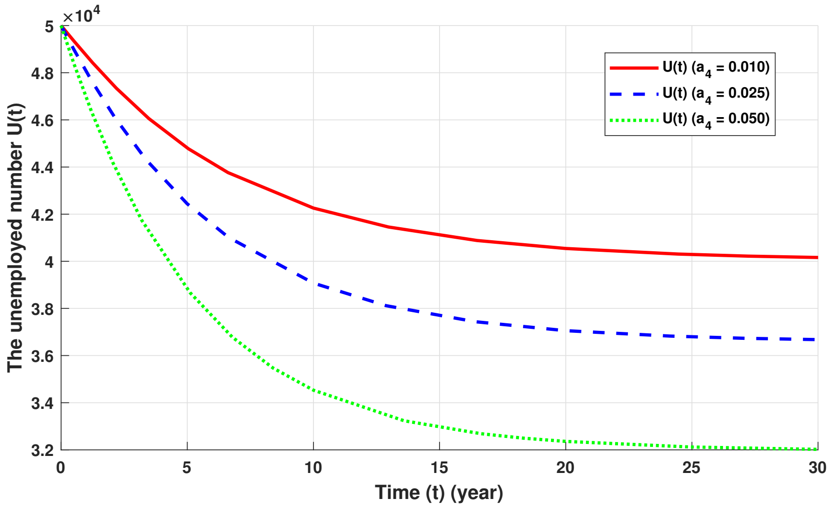

Figure 6. Impact of government support rate $a_4 \in \{0.010, 0.025, 0.050\}$ on the unemployed population $U(t)$ under Theorem 3.9 with $\tau = 10$. The downward shift in the equilibrium level validates the negative sensitivity index S_{U,a_4} as discussed in Table 2.

5.2. *Case study: Thailand's disability labor market (2022–2025)*

To evaluate the practical applicability and consistency of the proposed theoretical framework, this section applies the developed model to Thailand's disability labor market over a 16-quarter period. The model parameters are estimated using empirical data spanning the fiscal years 2022 to 2025 [27, 28]. An optimization algorithm is used for parameter estimation, while ensuring that the parameters satisfy conditions from the stability analysis. Due to missing or incomplete monthly records in certain periods during 2022-2023, the raw monthly data were preprocessed by calculating the quarterly average for each 3-month period to establish a consistent 16-quarter dataset. Detailed historical data prior to 2022 were unavailable on the public domains. For complete transparency, the full aggregated dataset, along with its variable definitions, is provided in Appendix A.

5.2.1. Case study 1: Global stability under Theorem 3.9

In this case study, we verify the asymptotic stability of the system under empirical conditions using 16 quarterly data sets. The initial condition was established based on the recorded statistics as the first quarter of the study period 2022.

$$\mathbf{x}_0 = \begin{bmatrix} U(0) \\ E(0) \\ V(0) \end{bmatrix} = \begin{bmatrix} 537,906 \\ 314,127 \\ 47,119 \end{bmatrix}.$$

To achieve a mathematically consistent fit, the model parameters were estimated via a constrained optimization process to satisfy the existence and stability conditions defined in Theorems 3.7 and 3.9. The optimized parameter set is summarized in Table 5.

Table 5. Parameter values satisfying conditions for Theorem 3.9 based on Thailand's 2022–2025 statistics.

Parameters	Values	Parameters	Values
a_1	31,981	b_2	0.039710
a_2	0.039710	b_3	0.00001
a_3	6.11×10^{-8}	c_1	0.025577
a_4	0.001632	c_2	0.574555
b_1	1×10^{-6}		

Under these parameters, the system converges to the equilibrium

$$E_p \approx [U^*, E^*, V^*]^\top = [737761, 67589, 32843]^\top.$$

The simulation results illustrated in Figure 7 demonstrate GA stability, confirming that the Thai disability labor market attains a stable steady state starting from the observed conditions in early 2022, independent of initial perturbations.

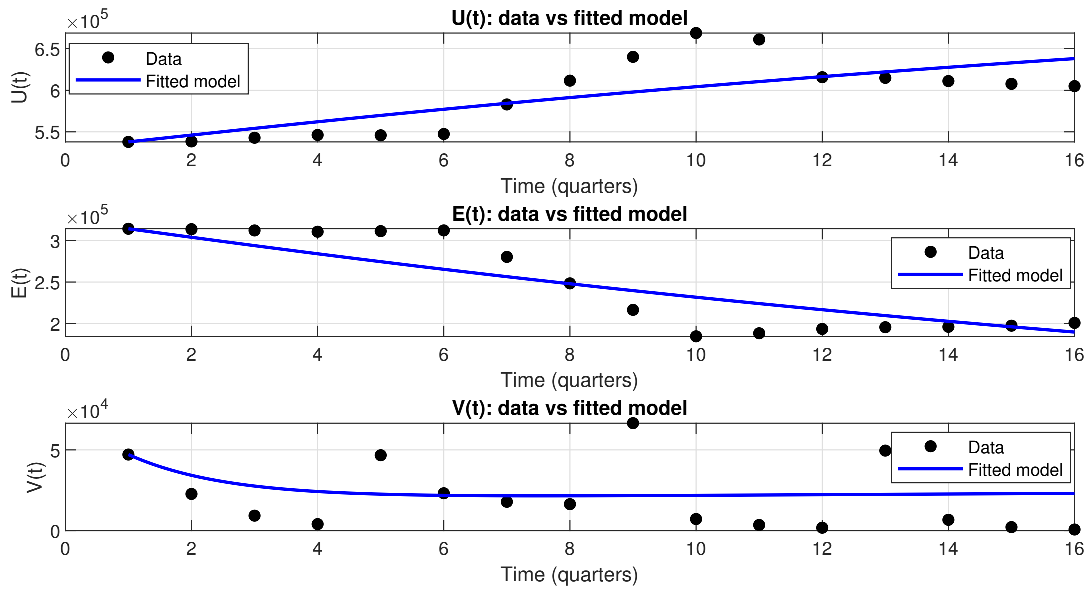

Figure 7. Model validation with empirical data.

5.2.2. Model with seasonal policy forcing

Empirical data from Thailand's disability labor market show a recurring increase in job vacancies at the beginning of each fiscal year, especially in January. This pattern is mainly driven by government policies, such as quota adjustments, financial incentives, and newly introduced employment programs. These actions create periodic shocks in the number of job vacancies, which cannot be captured by a standard time-invariant model.

To incorporate this phenomenon, we extend our proposed model by introducing a seasonal forcing term into the vacancy equation. The resulting system is given by

$$\begin{aligned}
\frac{dU(t)}{dt} &= a_1 - a_2U(t) - a_3U(t)V(t) - a_4U(t) + b_1E(t),\\
\frac{dE(t)}{dt} &= a_3U(t)V(t) + a_4U(t-\tau) - (b_1 + b_2)E(t),\\
\frac{dV(t)}{dt} &= (b_1 + b_3)E(t) + c_1U(t) - c_2V(t) + \eta S(t),
\end{aligned} \tag{5.1}$$

where $\tau > 0$ represents the implementation delay associated with training and job matching processes, and $\eta > 0$ quantifies the magnitude of the policy-driven increase in job vacancies.

The seasonal function $S(t)$ models periodic policy interventions and is defined as

$$S(t) = \sum_{k=0}^{\infty} \exp\left(-\frac{(t-4k)^2}{2\sigma^2}\right), \tag{5.2}$$

where $k \in \mathbb{N}_0$ is the integer index representing the successive fiscal year where each term in the summation corresponds to a policy intervention occurring at time $t = 4k$. The period of 4 corresponds to one year under quarterly time units. The parameter $\sigma > 0$ controls the temporal spread of each policy intervention, with smaller values representing short-term, concentrated effects and larger values corresponding to more persistent policy impacts.

To validate the proposed model, we implement empirical data from Thailand's disability labor market over a 16-quarter period (2022–2025) [27,28]. The initial condition is specified as

$$\mathbf{x}_0 = \begin{bmatrix} 537,906 \\ 314,127 \\ 47,119 \end{bmatrix},$$

representing the initial number of unemployed individuals, employed individuals, and job vacancies, respectively. The parameter vector is defined as

$$\mathbf{p} = (a_1, a_2, a_3, a_4, b_1, b_2, b_3, c_1, c_2, \eta).$$

Parameter estimation is formulated as a nonlinear least-squares problem:

$$\min_{\mathbf{p}} \sum_{i=1}^{N} \|\mathbf{x}_{\text{model}}(t_i;\mathbf{p}) - \mathbf{x}_{\text{data}}(t_i)\|_2^2, \tag{5.3}$$

where $\mathbf{x}_{\text{model}}(t_i;\mathbf{p})$ denotes the numerical solution of system (5.1) evaluated at observation times $\{t_i\}_{i=1}^{N}$.

Since the model is nonlinear and includes time delays, we solve it numerically using a DDE solver. The parameter estimation is carried out using a nonlinear optimization algorithm. To ensure that the model remains meaningful from both biological and economic perspectives, all parameters are restricted to be positive. In addition, the selected parameter values satisfy the stability conditions given in Theorems 3.7 and 3.9, ensuring that the system behaves consistently and remains dynamically stable.

Although the model contains a relatively large number of parameters compared with the 16 quarterly observations, the seasonal forcing term is introduced in a constrained structural form rather than as an unconstrained fitting component. Specifically, $S(t)$ is modeled as a Gaussian pulse train with a fixed period of 4 quarters, reflecting the annual fiscal and policy cycle observed in Thailand's disability labor market. Hence, the timing of the seasonal pulses is fixed *a priori*, and only the amplitude η and temporal spread σ are estimated. In addition, the remaining parameters are restricted to realistic ranges and are penalized if they violate the stability conditions derived in Theorem 3.9. These constraints reduce the effective parameter search space and help mitigate potential identifiability and overfitting concerns, although they do not completely eliminate them.

5.2.3. Error metrics and model validation

To evaluate the model's goodness-of-fit and predictive accuracy, multiple complementary error metrics are computed for each state variable.

- **Sum of squared errors (SSE):**

$$\mathrm{SSE} = \sum_{i=1}^{N} \sum_{j=1}^{3} \left(x_{j,\mathrm{model}}(t_i) - x_{j,\mathrm{data}}(t_i) \right)^2 .$$

- **Root mean square error (RMSE):**

$$\mathrm{RMSE} = \sqrt{\frac{1}{3N} \sum_{i=1}^{N} \sum_{j=1}^{3} \left(x_{j,\mathrm{model}}(t_i) - x_{j,\mathrm{data}}(t_i) \right)^2 }.$$

- **Mean absolute percentage error (MAPE):**

$$\mathrm{MAPE} = \frac{100}{3N} \sum_{i=1}^{N} \sum_{j=1}^{3} \left| \frac{x_{j,\mathrm{model}}(t_i) - x_{j,\mathrm{data}}(t_i)}{x_{j,\mathrm{data}}(t_i)} \right| .$$

These metrics provide a comprehensive assessment of model performance. The first one is SSE, which captures total deviation. The second is RMSE that reflects average prediction error magnitude, and MAPE offers a scale-independent measure suitable for cross-variable comparison.

The estimated parameter values are reported in Table 6. All parameters satisfy the theoretical stability conditions, ensuring that the fitted model remains dynamically well-posed.

Regarding the magnitudes of the estimated parameters in Table 6, some coefficients, such as a_3 and c_1, take very small values. This is partly due to the use of raw population counts rather than normalized proportions. Since $U(t)$ and $V(t)$ are measured as actual numbers of persons and vacancies, their product $U(t)V(t)$ can reach a magnitude of approximately 10^{10}. Consequently, the corresponding interaction coefficient a_3 must be small in order to produce realistic transition rates at the quarterly time scale. From an economic perspective, these small values also indicate low effective matching efficiency and strong structural frictions in the conventional employment pathway for persons with disabilities. Such frictions may arise from skill mismatches, workplace accessibility limitations, employer readiness, and administrative delays.

Table 6. Estimated parameter values satisfying the conditions of Theorem 3.9.

Parameter	Value	Parameter	Value
a_1	36,594	b_2	2.1066×10^{-5}
a_2	0.066001	b_3	0.063281
a_3	1.0151×10^{-12}	c_1	1.0004×10^{-6}
a_4	1.0249×10^{-6}	c_2	2.4466
b_1	0.036217	η	2×10^5

Figure 8(a) compares the model predictions with empirical data for all state variables. The results show that the refined model accurately captures the long-term trends in unemployment and employment. In addition, it successfully reproduces the sharp, periodic increases in job vacancies driven by policy interventions, and this improvement is achieved by including the seasonal forcing term. In particular, adding the seasonal forcing term enables the model to capture spike patterns in $V(t)$ that the previous model could not explain. Furthermore, Figure 8(b) presents sensitivity analysis with respect to the delay parameter τ. It indicates that

$$\tau = 4 \text{ quarters } = 12 \text{ months}$$

provides the best fit to the data. The final Figure 8(c) shows the seasonal forcing function $S(t)$, highlighting its role in generating periodic surges in job vacancies that are consistent with real-world policy cycles. For this choice of delay, the smallest fitting error among the tested values is shown in the following:

$$\text{SSE} = 4.011464 \times 10^{-1}, \quad \text{RMSE} = 21893.601384.$$

These experimental results suggest that the best temporal depiction of the dynamics of the disability labor market is a one-year delay ($\tau = 4$ quarters). In addition, the consequences of government employment policies, such as job matching, administrative procedures, and training, develop gradually over time rather than instantly. The projected 12-month delay is in accordance with yearly policy implementation cycles, in which employment results in later quarters are affected by vacancy increases announced at the start of the year.

The relatively small SSE value shows that the model with seasonal forcing fits the observed data well. The RMSE further indicates that the average prediction error is moderate compared to the scale of the data, since the numbers of unemployed and employed individuals are on the order of 10^5. Overall, the model successfully captures both the long-term trends in $U(t)$ and $E(t)$, as well as the recurring spike behavior in $V(t)$.

From the numerical results fitted to empirical data, it can be concluded that the proposed delay-seasonal model is not only mathematically consistent with the stability analysis but also aligns well with real-world labor market behavior.

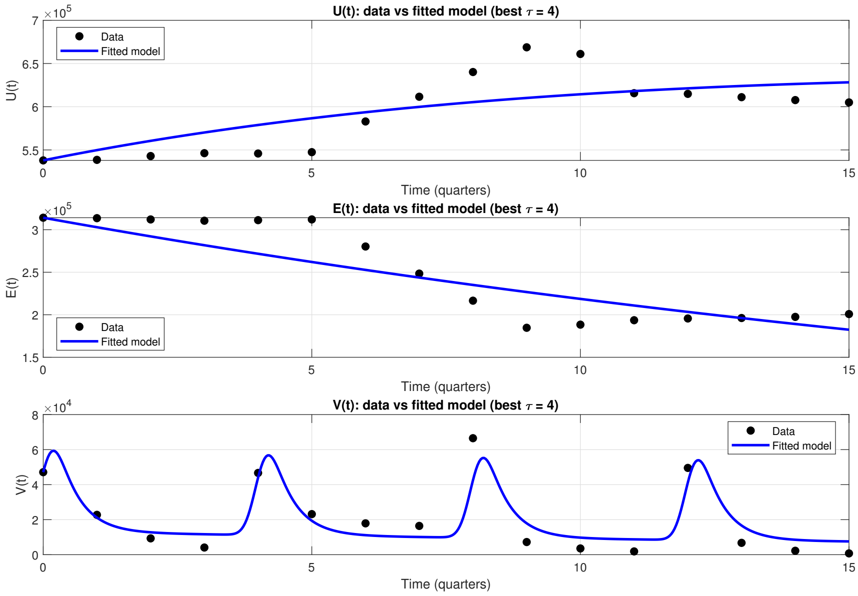

(**a**) Model vs. data

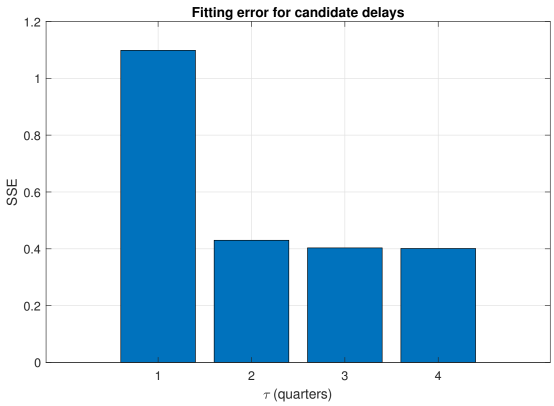

(**b**) Effect of delay τ

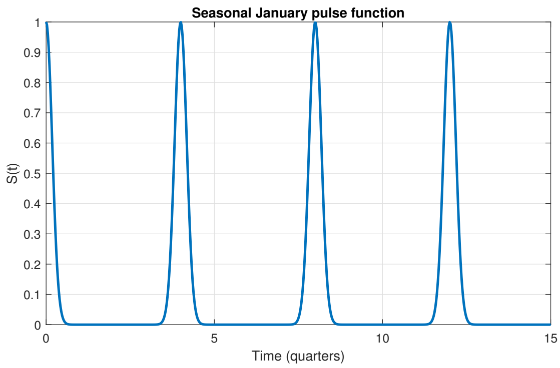

(**c**) Seasonal pulse function

Figure 8. Model validation and seasonal forcing analysis.

5.3. Numerical sensitivity results and policy implications

Building on the analytical framework developed in Section 4, this subsection presents a quantitative sensitivity analysis of the Thai disability labor market. Using the estimated parameter values in Table 5, we first compute the coefficients of the quadratic steady-state equation

$$\alpha(U^*)^2 + \beta U^* - \gamma = 0,$$

which characterizes the equilibrium level of unemployment.

The coefficients are given by

$$\alpha = a_3[b_2c_1 - a_2(b_1 + b_3)] = 6.2019172769 \times 10^{-11}, \quad (5.4)$$

$$\beta = a_1a_3(b_1 + b_3) + a_2c_2(b_1 + b_2) + a_4b_2c_2 = 9.4329418093 \times 10^{-4}, \quad (5.5)$$

$$\gamma = a_1c_2(b_1 + b_2) = 729.68885780. \quad (5.6)$$

The discriminant is computed as

$$\Delta = \beta^2 + 4\alpha\gamma = 1.0708227091 \times 10^{-6},$$

which confirms the existence of a unique positive equilibrium E_{p1}.

Solving the quadratic equation yields the steady-state value $U^* \approx 737{,}767$, representing the long-term unemployment level under the current market conditions. This value is used as the reference point for normalization in the sensitivity analysis.

The normalized SIs, denoted by $S_{U,p}$, are computed using (4.6) together with the analytical gradients derived in Section 4. These indices measure the relative impact of each parameter on the equilibrium unemployment level and are summarized in Table 7.

Table 7. Normalized SIs for the equilibrium E_{p1} based on Thailand's 2022–2025 statistics.

Parameters	**Derivative** ($\partial U^*/\partial p$)	**SI** ($S_{U,p}$)
a_1	$+2.2048 \times 10^1$	+0.95575578
a_2	-1.6266×10^7	−0.87553760
a_3	-5.3423×10^{11}	−0.04424422
a_4	-1.6266×10^7	−0.03597570
b_1	$+1.3734 \times 10^6$	+0.00000186
b_2	-5.1411×10^0	−0.00000028
b_3	-1.1693×10^5	−0.00000158
c_1	-1.2762×10^6	−0.04424248
c_2	$+5.6812 \times 10^4$	+0.04424422

The sensitivity results in Table 7 provide important insights into the dynamics of the Thai disability labor market. The sign of each sensitivity index (SI) is consistent with the model behavior. In particular, the positive SI of the inflow parameter a_1 indicates that an increase in the number of newly unemployed persons leads to a higher equilibrium unemployment level U^*. In contrast, the negative SI of the employment support parameter a_4 confirms that government interventions are effective in reducing unemployment at the steady state.

Among all parameters, a_1 has the largest sensitivity index ($S_{U,a_1} = +0.95575578$), making it the most influential factor. This implies that a 1% increase in the inflow of unemployed individuals results in an approximately 0.95575578% increase in U^*. This finding reflects a capacity-constrained labor market, where increases in the labor supply are not fully absorbed.

In addition, the system shows notable sensitivity to the job creation rate c_1 ($S_{U,c_1} = -0.04424248$) and the implementation rate of government support a_4 ($S_{U,a_4} = -0.03597570$), both of which contribute to reducing unemployment. The matching rate a_3 also has a negative effect ($S_{U,a_3} = -0.04424422$); however, its practical impact is limited due to the very small magnitude of its derivative.

Moreover, the vacancy closure rate c_2 ($S_{U,c_2} = +0.04424422$) has a stronger positive impact on unemployment than the layoff rate b_1 ($S_{U,b_1} = +0.00000186$), indicating that the loss of job vacancies plays a more critical role in increasing unemployment.

To sum up, these results suggest that policy efforts should prioritize increasing job creation (c_1), strengthening employment support programs (a_4), and maintaining existing vacancies (reducing c_2), rather than focusing solely on improving the matching efficiency (a_3), in order to achieve long-term labor market stability.

6. Conclusions

In this study, a mathematical model of the Thai disability labor market was developed using a DDE framework, providing a stronger structural and institutional justification for policy design by explicitly shifting from traditional memoryless systems to history-dependent dynamics, in which the dynamics of unemployed persons, employed persons, and job vacancies were investigated.

Both theoretical and numerical analyses were investigated. In particular, the theoretical analysis was integrated with empirical data from 2022 to 2025. It was shown that the equilibrium points E_{p1} and E_{p3} are GAS, independent of time delays. Numerical simulations confirmed that the system could autonomously recover from socioeconomic shocks, meaning that trajectories originating from a wide range of initial conditions converged to the corresponding equilibrium points. Even under large perturbations in unemployment, employment, and vacancy levels, the system returned to its steady state without requiring continuous external intervention, demonstrating strong global stability and resilience of the labor market structure.

To better capture empirical data from the Thai disability labor market, the model was extended by incorporating a seasonal forcing term $\eta S(t)$ into the vacancy equation. This extension enabled the model to reproduce the observed periodic spikes in job vacancies driven by annual government policy interventions. Numerical experiments showed that the delay-seasonal model provided a significantly improved fit to the empirical data, particularly in capturing the sharp fluctuations in $V(t)$ that the baseline model could explain.

Sensitivity analysis identified the inflow (a_1) and outflow (a_2) of unemployed persons as the dominant factors ($S_{U,a_1} = +0.95575578$, $S_{U,a_2} = -0.87553760$), indicating that labor supply dynamics played a central role in determining the equilibrium. In addition, the government support rate (a_4) and vacancy closure rate (c_2) exhibited greater influence than the employment rate (a_3), highlighting the importance of sustaining job vacancies alongside promoting job creation. Although long-term stability was preserved, administrative delays (τ) acted as systemic constraints that slowed convergence and prolonged recovery periods. The inclusion of this time delay allows the model to move beyond an idealized memoryless framework by capturing institutional lags in training, administrative processing, and job matching; although these delays do not alter long-term stability under the derived conditions, they significantly dictate transient oscillations and the speed of recovery toward the equilibrium state.

In summary, the proposed delay-seasonal model provided a robust and realistic framework for policy analysis in Thailand's disability labor market. The results suggested that achieving stability required not only increasing job opportunities but also improving administrative efficiency and maintaining vacancy levels to reduce implementation delays.

While the proposed delay-seasonal model provides a robust framework for policy analysis, certain limitations remain that open important avenues for future work. First, the present theoretical analysis focuses exclusively on delay-independent stability conditions; consequently, the rich bifurcation structure of the system outside these stable regions remains unexplored. Future research will investigate the critical delay thresholds and the existence of Hopf bifurcations to provide a deeper understanding of cyclical fluctuations in disability employment dynamics. Second, although focusing the sensitivity analysis on the steady state is well-motivated by the annual fiscal cycles of Thailand's disability employment policy, this static approach does not capture how parameter variations influence transient dynamics during short-term adjustment periods. Developing a time-dependent dynamic sensitivity analysis, alongside incorporating stochastic effects and skill-matching mechanisms, represents a critical next step to better capture the operational uncertainty and structural heterogeneity inherent in the labor market.

Ultimately, this framework sets itself apart from existing labor market models in the literature by breaking away from traditional ordinary differential equation (ODE) structures that incorrectly assume instantaneous workforce adjustments. While classic models overlook temporal gaps, our delay-seasonal DDE model successfully isolates administrative and retraining lags (τ) as systemic constraints, proving that policy efficacy is strictly bounded by these delays. By bridging nonlinear global stability with the 16-quarter empirical reality of Thailand's post-COVID-19 recovery phase, this model provides an advanced computational tool that moves beyond abstract theory, offering tangible predictive power to safeguard vulnerable labor segments against structural decay.

Author contributions

P. Chanosot: Conceptualization, methodology, software, and writing - original draft. **S. Wongkaew**: Formal analysis, validation, numerical experiments, writing- review and editing. **T. Petaratip**: Formal analysis and validation. **P. Niamsup**: Supervision, project administration, and funding acquisition. All authors reviewed the results and approved the final version of the manuscript.

Use of Generative-AI tools declaration

The authors declare that they have used artificial intelligence (AI) tools, specifically Gemini and ChatGPT, during the preparation of this article. These tools were utilized solely to assist in improving English grammar, refining sentence structures, and enhancing the overall linguistic clarity and LaTeX formatting of the manuscript. This AI assistance was applied throughout the entire text during the final drafting and proofreading stages. No scientific content, mathematical modeling, or numerical data was generated or altered by the AI tools, and the authors maintain full responsibility for the final contents of the published work.

Acknowledgments

This work was supported by Chiang Mai University. The first author gratefully acknowledges the TA/RA Scholarship from the Graduate School at Chiang Mai University (CMU). The authors thank the Department of Employment (DEP) and the National Statistical Office (NSO) of Thailand for providing the labor market data. They also extend their appreciation to the editors and anonymous reviewers for their constructive suggestions.

Conflict of interest

The authors declare that they have no known competing financial interests or personal relationships that could have appeared to influence the work reported in this paper.

References

1. S. Al-Sheikh, R. Al-Maalwi, H. A. Ashi, A mathematical model of unemployment with the effect of limited jobs, *Comptes Rendus. Math.*, **359** (2021), 283–290. https://doi.org/10.5802/crmath.164
2. G. N. Pathan, P. H. Bhathawala, A mathematical model for unemployment with effect of self employment, *IOSR J. Math.*, **11** (2015), 37–43.
3. H. Yang, Analyzing global stability of the delay viral model with general incidence rate, *Differ. Equ. Dyn. Syst.*, **24** (2016), 319–328. https://doi.org/10.1007/s12591-016-0295-9
4. P. Chanosot, S. Wongkaew, *Stability analysis of unemployment model in Thailand after COVID-19 outbreak*, MS. Thesis, Chiang Mai University, 2022.
5. A. K. Misra, A. K. Singh, A delay mathematical model for the control of unemployment, *Differ. Equ. Dyn. Syst.*, **21** (2013), 291–307. https://doi.org/10.1007/s12591-012-0153-3
6. T. Petaratip, P. Niamsup, Stability analysis of an unemployment model with time delay, *AIMS Math.*, **6** (2021), 7421–7440. https://doi.org/10.3934/math.2021434
7. A. K. Misra, M. Kumari, M. Sajid, Role of informal sector to combat unemployment in developing economy: a modeling study, *Heliyon*, **10** (2024), e33378. https://doi.org/10.1016/j.heliyon.2024.e33378
8. P. K. Singh, K. Lata, A. K. Singh, A. K. Misra, Modeling the effect of unemployment augmented industrialization on the control of unemployment, *Environ. Dev. Sustain.*, **25** (2023), 587–600. https://doi.org/10.1007/s10668-021-02069-6
9. S. B. Munoli, S. Gani, S. R. Gani, A mathematical approach to employment policies: an optimal control analysis, *Int. J. Stat. Syst.*, **12** (2017), 549–565.
10. S. B. Munoli, S. Gani, Optimal control analysis of a mathematical model for unemployment, *Optim. Control Appl. Methods*, **37** (2016), 798–806. https://doi.org/10.1002/oca.2195

11. S. A. Somma, R. O. Omotinuwe, N. O. Abdurrahman, Mathematical model for the control of unemployment in Nigeria incorporating vocational education and apprenticeship, *Al-Mustansiriyah J. Sci.*, **36** (2025), 1–17. https://doi.org/10.23851/mjs.v36i2.1655

12. A. K. Misra, A. K. Singh, A mathematical model for unemployment, *Nonlinear Anal.*, **12** (2011), 128–136. https://doi.org/10.1016/j.nonrwa.2010.06.002

13. L. Harding, M. Neamţu, A dynamic model of unemployment with migration and delayed policy intervention, *Comput. Econ.*, **51** (2018), 427–462. https://doi.org/10.1007/s10614-016-9610-3

14. Z. Aamer, S. Jawad, B. Batiha, A. H. Ali, F. Ghanim, A. A. Lupaş, Evaluation of the dynamics of psychological panic factor, glucose risk and estrogen effects on breast cancer model, *Computation*, **12** (2024), 160. https://doi.org/10.3390/computation12080160

15. M. Ahmed, S. Jawad, The role of antibiotics and probiotics supplements on the stability of gut flora bacteria interactions, *Commun. Math. Biol. Neurosci.*, **2023** (2023), 33.

16. E. Hakeem, S. Jawad, A. H. Ali, M. Kallel, H. A. Neamah, How mathematical models might predict desertification from global warming and dust pollutants, *MethodsX*, **14** (2025), 103259. https://doi.org/10.1016/j.mex.2025.103259

17. J. K. Hale, *Ordinary differential equations*, Courier Corporation, 2009.

18. M. W. Hirsch, S. Smale, R. L. Devaney, *Differential equations, dynamical systems, and an introduction to chaos*, 3 Eds., Academic Press, 2013. https://doi.org/10.1016/C2009-0-61160-0

19. J. K. Hale, S. M. V. Lunel, *Introduction to functional differential equations*, Vol. 99, Springer Science & Business Media, 2013.

20. H. Smith, *An introduction to delay differential equations with applications to the life sciences*, Vol. 57, Springer New York, 2011. https://doi.org/10.1007/978-1-4419-7646-8

21. H. K. Khalil, J. W. Grizzle, *Nonlinear systems*, Vol. 3, Upper Saddle River, Prentice Hall, 2002.

22. A. Patil, Routh-Hurwitz criterion for stability: an overview and its implementation on characteristic equation vectors using MATLAB, In: A. E. Hassanien, S. Bhattacharyya, S. Chakrabati, A. Bhattacharya, S. Dutta, *Emerging technologies in data mining and information security*, Advances in Intelligent Systems and Computing, Springer, Singapore, **1286** (2021), 319–329. https://doi.org/10.1007/978-981-15-9927-9_32

23. S. Ruan, J. Wei, On the zeros of a third degree exponential polynomial with applications to a delayed model for the control of testosterone secretion, *IMA J. Math. Appl. Med. Biol.*, **18** (2001), 41–52. https://doi.org/10.1093/imammb/18.1.41

24. L. Perko, *Differential equations and dynamical systems*, Vol. 7, Springer Science & Business Media, 2013.

25. J. P. La Salle, *The stability of dynamical systems*, Society for Industrial and Applied Mathematics, 1976.

26. L. Arriola, J. M. Hyman, Sensitivity analysis for uncertainty quantification in mathematical models, In: G. Chowell, J. M. Hyman, L. M. A. Bettencourt, C. Castillo-Chavez, *Mathematical and statistical estimation approaches in epidemiology*, Springer, 2009, 195–247. https://doi.org/10.1007/978-90-481-2313-1_10

27. Department of Empowerment of Persons with Disabilities, Report on the situation of persons with disabilities in Thailand, Ministry of Social Development and Human Security (Data retrieved as of March 31, 2025), 2025.

28. National Statistical Office of Thailand, The 2025 disability survey, Ministry of Digital Economy and Society, Quarterly Labor Force Statistics, 2025.

29. N. Chitnis, J. M. Hyman, J. M. Cushing, Determining important parameters in the spread of malaria through the sensitivity analysis of a mathematical model, *Bull. Math. Biol.*, **70** (2008), 1272–1296. https://doi.org/10.1007/s11538-008-9299-0

Appendix

A. Detailed proof of Theorem 3.9

In this appendix, we provide the exhaustive, step-by-step mathematical derivation for the GA stability of the interior equilibrium point $E_{p1}(U_1, E_1, V_1)$, as stated in Theorem 3.9.

To conduct this global analysis, we define a positive-definite Goh-Volterra-Lyapunov functional candidate $W_1(t)$ incorporating a delayed history integral as follows:

$$W_1(t) = U_1 g\left(\frac{U}{U_1}\right) + E_1 g\left(\frac{E}{E_1}\right) + V_1 g\left(\frac{V}{V_1}\right) + a_4 U_1 \int_{t-\tau}^{t} \frac{U(s)}{U_1} ds. \tag{A.1}$$

Differentiating $W_1(t)$ along the solution trajectories with respect to time t via the Leibniz integral rule yields:

$$\frac{dW_1}{dt} = \left(1 - \frac{U_1}{U}\right)\dot{U} + \left(1 - \frac{E_1}{E}\right)\dot{E} + \left(1 - \frac{V_1}{V}\right)\dot{V} + a_4 U_1 \left[g\left(\frac{U}{U_1}\right) - g\left(\frac{U(t-\tau)}{U_1}\right)\right]. \tag{A.2}$$

To ensure complete transparency, we expand each structural component of Eq (A.2) individually by embedding the steady-state identities:

$$\begin{aligned}\left(1 - \frac{U_1}{U}\right)\dot{U} =& -(a_2 + a_4)U_1 g\left(\frac{U}{U_1}\right) - a_1 g\left(\frac{U_1}{U}\right) + b_1 E_1 g\left(\frac{E}{E_1}\right) \\ &+ a_3 U_1 V_1 g\left(\frac{V}{V_1}\right) - a_3 U_1 V_1 g\left(\frac{UV}{U_1 V_1}\right) - b_1 E_1 g\left(\frac{U_1 E}{U E_1}\right),\end{aligned} \tag{A.3}$$

$$\begin{aligned}\left(1 - \frac{E_1}{E}\right)\dot{E} =& -(a_3 U_1 V_1 + a_4 U_1) g\left(\frac{E}{E_1}\right) + a_3 U_1 V_1 g\left(\frac{UV}{U_1 V_1}\right) + a_4 U_1 g\left(\frac{U(t-\tau)}{U_1}\right) \\ &- a_4 U_1 g\left(\frac{E_1 U(t-\tau)}{E U_1}\right) - a_3 U_1 V_1 g\left(\frac{E_1 U V}{E U_1 V_1}\right),\end{aligned} \tag{A.4}$$

$$\begin{aligned}\left(1 - \frac{V_1}{V}\right)\dot{V} =& c_1 U_1 g\left(\frac{U}{U_1}\right) + (b_1 + b_3) E_1 g\left(\frac{E}{E_1}\right) - c_2 V_1 g\left(\frac{V}{V_1}\right) \\ &- c_1 U_1 g\left(\frac{V_1 U}{V U_1}\right) - (b_1 + b_3) E_1 g\left(\frac{V_1 E}{V E_1}\right).\end{aligned} \tag{A.5}$$

Summing these individual expansions together, the cross-transmission terms $+a_3 U_1 V_1 g\left(\frac{UV}{U_1 V_1}\right)$ and $-a_3 U_1 V_1 g\left(\frac{UV}{U_1 V_1}\right)$ cancel out perfectly. Collecting the remaining coefficients leads to:

$$\begin{aligned}\frac{dW_1}{dt} =& (-a_2 + c_1)\, U_1 g\left(\frac{U}{U_1}\right) + (-b_2 + b_1 + b_3)\, E_1 g\left(\frac{E}{E_1}\right) + (a_3 U_1 - c_2)\, V_1 g\left(\frac{V}{V_1}\right) \\ & - a_1 g\left(\frac{U_1}{U}\right) - b_1 E_1 g\left(\frac{U_1 E}{U E_1}\right) - a_4 U_1 g\left(\frac{E_1 U(t-\tau)}{E U_1}\right) \\ & - a_3 U_1 V_1 g\left(\frac{E_1 UV}{E U_1 V_1}\right) - c_1 U_1 g\left(\frac{V_1 U}{V U_1}\right) - (b_1 + b_3) E_1 g\left(\frac{V_1 E}{V E_1}\right). \end{aligned} \tag{A.6}$$

Since $g(x) \geq 0$ for all $x > 0$, under the sufficient conditions $a_2 \geq c_1$, $b_2 \geq b_1 + b_3$, and $c_2 \geq a_3 U_1$, we guarantee that $dW_1/dt \leq 0$. By LaSalle's invariance principle, every positive solution converges globally asymptotically to E_{p1}.

B. Detailed proof of Theorem 3.10

In this appendix, we provide the complete step-by-step mathematical expansion for the GA stability of the boundary/interior equilibrium point $E_{p3}(U_3, E_3, V_3)$ when $\alpha = 0$, as stated in Theorem 3.10.

We define the corresponding Lyapunov-Krasovskii functional candidate $W_3(t)$ as follows:

$$W_3(t) = U_3 g\left(\frac{U}{U_3}\right) + E_3 g\left(\frac{E}{E_3}\right) + V_3 g\left(\frac{V}{V_3}\right) + a_4 U_3 \int_{t-\tau}^{t} g\left(\frac{U(s)}{U_3}\right) ds. \tag{B.1}$$

Differentiating $W_3(t)$ along the solution trajectories with respect to time t yields:

$$\frac{dW_3}{dt} = \left(1 - \frac{U_3}{U}\right)\dot{U} + \left(1 - \frac{E_3}{E}\right)\dot{E} + \left(1 - \frac{V_3}{V}\right)\dot{V} + a_4 U_3 \left[g\left(\frac{U}{U_3}\right) - g\left(\frac{U(t-\tau)}{U_3}\right)\right]. \tag{B.2}$$

By executing algebraic expansions and cross-term cancellations structurally identical to the derivations in Appendix A, the total time derivative simplifies to:

$$\begin{aligned}\frac{dW_3}{dt} =& (-a_2 + c_1)\, U_3 g\left(\frac{U}{U_3}\right) + (-b_2 + b_1 + b_3)\, E_3 g\left(\frac{E}{E_3}\right) + (a_3 U_3 - c_2)\, V_3 g\left(\frac{V}{V_3}\right) \\ & - a_1 g\left(\frac{U_3}{U}\right) - b_1 E_3 g\left(\frac{U_3 E}{U E_3}\right) - a_4 U_3 g\left(\frac{E_3 U(t-\tau)}{E U_3}\right) \\ & - a_3 U_3 V_3 g\left(\frac{E_3 UV}{E U_3 V_3}\right) - c_1 U_3 g\left(\frac{V_3 U}{V U_3}\right) - (b_1 + b_3) E_3 g\left(\frac{V_3 E}{V E_3}\right). \end{aligned} \tag{B.3}$$

Under the identical parameter conditions $a_2 \geq c_1$, $b_2 \geq b_1 + b_3$, and $c_2 \geq a_3 U_3$, it follows that $dW_3/dt \leq 0$ holds strictly across the positive orthant. By LaSalle's invariance principle, the largest invariant set contained within $dW_3/dt = 0$ is the singleton $\{E_{p3}\}$. This completes the proof.